



12-1982

## **Seasat Orbital Radar Imagery Applied to Lineament Analysis and Relationships with Hydrocarbon Production in the Wartburg Basin Area, Tennessee**

S. E. A. Brite

*University of Tennessee - Knoxville*

Follow this and additional works at: [https://trace.tennessee.edu/utk\\_gradthes](https://trace.tennessee.edu/utk_gradthes)



Part of the [Geology Commons](#)

---

### **Recommended Citation**

Brite, S. E. A., "Seasat Orbital Radar Imagery Applied to Lineament Analysis and Relationships with Hydrocarbon Production in the Wartburg Basin Area, Tennessee." Master's Thesis, University of Tennessee, 1982.

[https://trace.tennessee.edu/utk\\_gradthes/850](https://trace.tennessee.edu/utk_gradthes/850)

This Thesis is brought to you for free and open access by the Graduate School at TRACE: Tennessee Research and Creative Exchange. It has been accepted for inclusion in Masters Theses by an authorized administrator of TRACE: Tennessee Research and Creative Exchange. For more information, please contact [trace@utk.edu](mailto:trace@utk.edu).

To the Graduate Council:

I am submitting herewith a thesis written by S. E. A. Brite entitled "Seasat Orbital Radar Imagery Applied to Lineament Analysis and Relationships with Hydrocarbon Production in the Wartburg Basin Area, Tennessee." I have examined the final electronic copy of this thesis for form and content and recommend that it be accepted in partial fulfillment of the requirements for the degree of Master of Science, with a major in Geography.

G. Michael Clark, Major Professor

We have read this thesis and recommend its acceptance:

Don W. Byerly, John B. Rehder

Accepted for the Council:

Carolyn R. Hodges

Vice Provost and Dean of the Graduate School

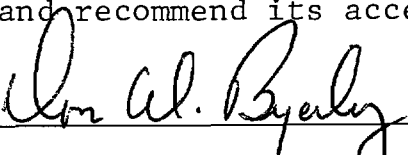
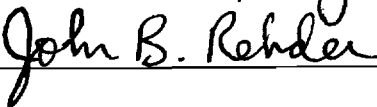
(Original signatures are on file with official student records.)

To the Graduate Council:


I am submitting herewith a thesis written by S.E.A. Brite entitled "Seasat Orbital Radar Imagery Applied to Lineament Analysis and Relationships with Hydrocarbon Production in the Wartburg Basin Area, Tennessee." I have examined the final copy of this thesis for form and content and recommend that it be accepted in partial fulfillment of the requirements for the degree of Master of Science, with a major in Geology.

  
G. Michael Clark, Major Professor

We have read this thesis  
and recommend its acceptance:

Accepted for the Council:

  
Vice Chancellor  
Graduate Studies and Research

SEASAT ORBITAL RADAR IMAGERY APPLIED TO LINEAMENT  
ANALYSIS AND RELATIONSHIPS WITH HYDROCARBON  
PRODUCTION IN THE WARTBURG BASIN AREA,  
TENNESSEE

A Thesis  
Presented for the  
Master of Science  
Degree  
The University of Tennessee, Knoxville

S.E.A. Brite  
December 1982

**3065140**

## ACKNOWLEDGMENTS

I thank Dr. G. Michael Clark for suggesting the subject of this thesis and for his support and guidance throughout this investigation. I also thank the other members of my thesis committee, Dr. Don W. Byerly and Dr. John B. Rehder, for reading this manuscript and for their very professional critique of this thesis.

I would also like to thank Dr. John Ford of the Jet Propulsion Lab in Pasadena, California for supplying much of the Seasat data used. I wish to acknowledge the Geological Society of America for partially funding this research project with Research Grant Number 4845M awarded in April, 1980. My thanks to the Tennessee Oil and Gas Association for their interest in this analysis.

## ABSTRACT

Seasat, an orbital synthetic aperture radar launched in 1978, has produced high-resolution imagery enhancing over 1186 observed linear topographic indentations or lineaments in the Wartburg Basin area of east-central Tennessee. The main objectives of this thesis are to verify these lineaments in the field, to compare them with aerial photographic lineaments in the same area, to statistically analyze lineament trends, and to compare lineaments with oil and gas trends in the Wartburg Basin area.

Lineaments from Seasat imagery were located in the field with a high degree of accuracy. Three distinct lineament systems were derived from lineament orientations, their grouping and continuity. There are two basic types of lineaments on the imagery, long lineaments that extend for distances over 40 km and shorter subparallel lineaments usually no longer than 4 km. 40% of the longer lineaments are parallel to drainage. Of the total 1186 lineaments, 40% are terminated by crosscutting lineaments. 57% of the total lineaments are related to aeromagnetic and gravity contours indicating a possible basement relationship. The longer lineaments possibly represent major bedrock penetrating fracture zones along which hydrocarbons disperse. Oil and gas wells farther from the lineament zones had a slight increase in initial hydrocarbon production, wellhead pressure

and subsurface fracturing. This could indicate that future wellsites should be chosen away from major lineament zones.

## TABLE OF CONTENTS

CHAPTER	PAGE
I. INTRODUCTION . . . . .	1
General Discussion . . . . .	1
Thesis Objectives . . . . .	3
Choosing the Study Area . . . . .	3
Rationale for Using Seasat Imagery . . . . .	4
Significance of Lineaments . . . . .	5
II. THE RESEARCH AREA . . . . .	7
General Physiographic Setting . . . . .	7
Location of the Study Area . . . . .	8
Stratigraphy . . . . .	9
Structure . . . . .	11
III. INTERPRETING SEASAT IMAGERY . . . . .	13
Radar Return Characteristics . . . . .	13
Picture Elements and Resolution . . . . .	13
Distortions . . . . .	14
Lineaments on the Imagery . . . . .	16
Analysis Techniques and Materials Required . . . . .	18
IV. FIELD DATA ACQUISITION . . . . .	21
Locating Lineaments in the Field . . . . .	21
V. COMPARATIVE ANALYSIS OF LINEAMENTS IN THE STUDY AREA . . . . .	37
Seasat Imagery Compared to Aerial Photographic Imagery . . . . .	37
General Study Area Analysis: Four Lineament Systems . . . . .	47
VI. HYDROCARBONS AND LINEAMENTS . . . . .	63
Introduction . . . . .	63
Phase 1: General Analysis of Production in 594 Wells . . . . .	63
Phase 2: Analysis of Gas and Oil Production in 308 Wells . . . . .	65
Phase 3: Subsurface Fracturing in Relation to Lineaments . . . . .	72



CHAPTER	PAGE
VII. CONCLUSIONS . . . . .	81
LIST OF REFERENCES . . . . .	84
APPENDIX . . . . .	89
VITA . . . . .	93

## LIST OF TABLES

TABLE	PAGE
1. Comparison of Average Lineament Lengths on Seasat Imagery to Average Lineament Lengths on Aerial Photographic Imagery . . . . .	39
2. Comparison of the Number of Lineaments and Lineament Lengths from Seasat Imagery which Correspond to Lineaments on Aerial Photographic Imagery . . . . .	41
3. Comparison of Probable Lineaments and Lineament Lengths from Seasat Imagery which Correspond to Lineaments on Aerial Photographic Imagery . . . . .	42
4. Seasat Lineament Terminations Compared to Aerial Photographic Lineament Terminations . . . . .	45
5. Breakdown of 1186 Lineaments into Four Systems . . . . .	47
6. Comparison of Average Lineament Lengths in the Four Systems . . . . .	50
7. Comparison of Lineaments Parallel to Drainage with Respect to Distance . . . . .	53
8. Comparison of Lineaments Terminated by Drainage . . . . .	54
9. Comparison of Lineaments Terminated by Other Lineaments . . . . .	57
10. Comparison of Lineaments Aligned with Gravity Contours . . . . .	60
11. Comparison of Lineaments Related to Aeromagnetic Contours . . . . .	61
12. Comparison of Wells Over 500 Ft. From a Lineament to Wells Within 500 ft. of a Lineament . . . . .	65
13. Comparison of Oil Production in Wells With Respect to Distance From Lineaments . . . . .	67

TABLE	PAGE
14. Comparison of Gas Production in Wells With Respect to Distance From Lineaments . . . . .	69
15. Comparison of Oil Wellhead Pressure With Respect to Well Distance From a Lineament . . .	70
16. Comparison of Gas Wellhead Pressure With Respect to Well Distance From a Lineament . . .	72
17. Comparison of Well Fractures With Respect to Distances From Lineaments . . . . .	77
18. Comparison of Well Fractures Containing Oil and Gas With Respect to Distances From Lineaments . . . . .	78
19. Comparison of Well Fractures With Lineament Orientations . . . . .	80
20. Comparison of Well Fractures Containing Oil and Gas With Lineament Orientations . . . . .	80

## LIST OF FIGURES

FIGURE	PAGE
1. Seasat Bus and Payload Configuration (After Ford et al., 1980) . . . . .	2
2. Location and Extent of the Project Area Covered by Seasat . . . . .	8
3. Location of the Study Area . . . . .	9
4. Generalized Stratigraphic Sequence of Pennsylvanian Rocks in the Wartburg Basin Area (After Luther, 1959) . . . . .	10
5. Revisions in the Nomenclature Proposed by Barlow (1969) . . . . .	11
6. Structural Features of the Wartburg Basin Area (After Luther, 1959) . . . . .	12
7. Seasat Imaging Geometry Shown to Scale in Elevation View (After Ford, 1980) . . . . .	14
8. Common Distortions on Seasat Imagery . . . . .	15
9. Examples of Basic Lineament Types . . . . .	17
10. 1186 Tonal and Textural Lineaments on Seasat Imagery of the Wartburg Basin Area . . . . .	19
11. 71 Field Stations That Were Checked for Lineaments . . . . .	22
12. Field Station 49 . . . . .	24
13. Field Station 24 . . . . .	26
14. Parallel Fractures at Field Station 55 . . . . .	27
15. Closer View of One of the Fractures at Field Station 55 . . . . .	28
16. View to Northwest at Station 52 . . . . .	29
17. Example 5: Field Station 52 . . . . .	30
18. Example 6: Field Station 7 . . . . .	32

FIGURE	PAGE
19. Example 7: Field Station 42 . . . . .	35
20. Drilling Activity Within 100 Feet (30m) of the Projected Lineament in Example 7 . . . . .	36
21. Matching Lineaments (Solid Lines) From the Combined Imagery . . . . .	40
22. Lineaments Terminated by Crosscutting Lineaments From the Combined Imagery . . . . .	44
23. Aerial Photographic Lineaments (Darker Lines) Compared to Seasat Lineaments . . . . .	46
24. Rose Diagram of the Four Lineament Systems . . . . .	48
25. The Four Lineament Systems in the General Study Area . . . . .	51
26. Lineaments Terminated by Drainage . . . . .	55
27. Lineaments Terminated by Crosscutting Lineaments . . . . .	56
28. Lineaments Related to Gravity Contours . . . . .	59
29. Lineaments Aligned with Aeromagnetic Contours . . . . .	62
30. Study Area for Phase 1 (Blocks A and B) . . . . .	64
31. Initial Oil and Gas Well Production Averages . . . . .	67
32. Initial Wellhead Pressure Averages . . . . .	71
33. Map Showing the Locations of 25 Wells Analyzed for Fracturing at Depth . . . . .	74
34. Average Fractures and Pay Fractures per Well in Relation to Distance From a Lineament . . . . .	77

## CHAPTER I

### INTRODUCTION

#### I. GENERAL DISCUSSION

Seasat, a new type of radar satellite, was placed into Earth orbit on June 29, 1978. From over 500 miles (804km) in space, Seasat can detect objects on the surface as small as 45 feet (13.7m) in length. This is three times the imaging capability of any previous satellite. One of Seasat's most important uses was to detect linear topographic indentations or lineaments on the Earth. These consist mainly of "...topographic (including straight stream segments), vegetation or soil tonal alignments...expressed continuously or discontinuously for many miles..." (Lattman, 1958). Other linear features in the study area include faults, master joint sets in bedrock exposures, and closely spaced bedrock fractures. Often straight stream segments correspond with wind and water gaps across ridges (Ford, 1980). Man-made linear features on the imagery include roads, railroads, cultivated areas, power lines, and strip-mined areas. A brief explanation of terms which are commonly employed in remote sensing is provided in the appendix.

Seasat, which was a joint effort of NASA and the Jet Propulsion Lab of Pasadena, California, circled the Earth 14 times daily at an altitude of 500 miles (804km) in a

near-polar circular orbit. The satellite operated on the L band, a microwave 23.5 cm in length. Along with its synthetic aperture radar (SAR) Seasat carried an array of instruments to monitor the Earth (Figure 1). Although Seasat's primary mission was to monitor the Earth's oceans, it also produced highly detailed imagery as it passed over land. After three and one-half months, an electrical short circuit disabled the satellite ending transmissions on October 10, 1978. In this brief period, Seasat provided about 2500 minutes of operation producing images of over 38.6 million square miles (100 million sq km) of the Earth's surface. Seasat imagery is now publicly available thru NOAA (1981) and is becoming a valuable tool for terrane analysis.

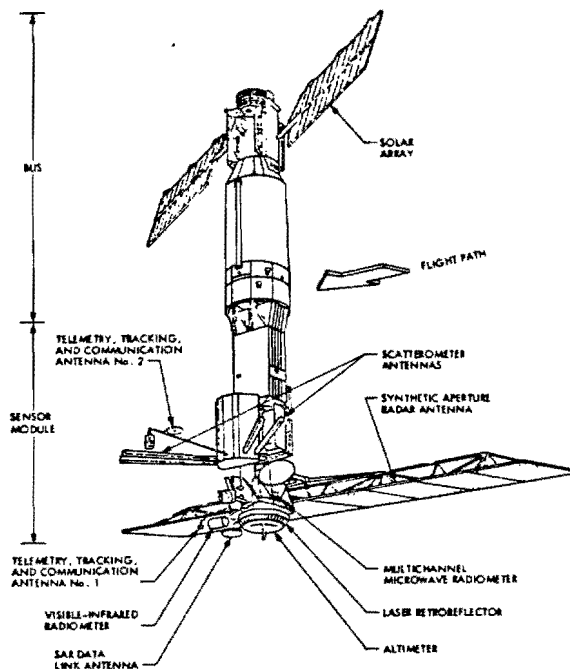


Figure 1. Seasat bus and payload configuration. (After Ford et al., 1980)

## II. THESIS OBJECTIVES

The main objectives of this thesis are to:

1. Determine lineaments on Seasat imagery and verify them in the field
2. Analyze lineament trends statistically to determine their relationship to major drainage, to aeromagnetic and gravity trends, and to the general topography
3. Compare Seasat lineaments with two aerial photographic lineament studies in the same area (Slusarski, 1979 and Masuoka, 1981)
4. Analyze lineament trends in relation to oil and gas trends, including well production, wellhead production pressure, and subsurface fracturing in wells.

## III. CHOOSING THE STUDY AREA

The Wartburg Basin is a rapidly developing hydrocarbon resource area. A lineament analysis in this area could be useful in oil and gas exploration. Smith and Drahovzal (1972) have suggested that linear trends could represent bedrock penetrating fracture zones which act as migration channels for the concentration or dispersal of hydrocarbon deposits.

Lineaments in the Wartburg Basin area have been analyzed



by Slusarski (1979) and Masuoka (1981) using aerial photographic imagery. This provides an opportunity to compare Seasat lineaments with aerial photographic lineaments.

#### IV. RATIONALE FOR USING SEASAT IMAGERY

Almost 40% of the Wartburg Basin has limited road access with steep terrane and dense vegetation. Seasat imagery is excellent for the regional assessment of linear trends in this type of area. Although Seasat does not penetrate a heavy vegetative cover, it is able to pick up linear indentations in the vegetative canopy which can represent bedrock fracture zones (Ford, 1980). Seasat can penetrate heavy cloud cover, fog, even light rain and needs no illumination source. Seasat also detects slight planar angle changes in the topography which often represent changes in lithology. Changes in vegetation, soil texture, soil content, and surface and near-surface moisture also show up on the imagery. These features combine to form a surface dielectric constant which Seasat detects (Elachi, 1980). The dielectric constant of a medium is defined as the propagation characteristics of an electromagnetic wave through the medium (Schmugge, 1980). Abrupt changes in the dielectric constant are often found in lineament zones.

Seasat imagery has been compared to Landsat imagery, to side looking airborne radar imagery, and to aerial photographic imagery (Ford, 1980, Daily et al., 1979, Hardaway et al., 1982 and Foster et al., 1981). Presently no other type of

remote sensing system produces imagery like Seasat. If lineaments on Seasat imagery are compared to lineaments on these other types of imagery, it may add a new dimension to terrane analysis.

## V. SIGNIFICANCE OF LINEAMENTS

Blanchet (1957) states that the analytical exploration technique known as fracture analysis is based on the concept that the Earth's crust is abundantly and systematically fractured. Hobbs (1911) defined lineaments as "significant lines in the Earth's surface" and proposed a system of fractures on a continental scale, oriented northwest to southeast and northeast to southwest with a minor fracture system oriented north to south and east to west. Deviations from the basic orientations were thought to be the result of local structural influences. The concept of Hobbs' basic orientations has not changed to the present time.

E.P. Kaiser (1950) states that lineaments are thought to be passive structures produced by recurrent movement of basement blocks. Blanchet (1957) attributes this movement to flexing caused by earth tides which propagate as deep set fractures moving upward to the surface, even through unconsolidated soils and glacial overburden. Close parallels between the orientation of basic units of jointing and lineament orientations have been found in the Appalachian Plateau of Pennsylvania by Nickelson and Hough (1967) and Lattman

and Nickelson (1958). Nickelson and Hough noted two types of bedrock jointing, systematic jointing and nonsystematic jointing. Systematic joints are defined as extension fractures formed perpendicular to the direction of least compression in the presence of suitable fluid pressure overburden weight ratios (Secor, 1965). Nonsystematic joints are extension fractures of late release origin caused by unloading of the overburden sediment load. The two types of joints were found to intersect at approximately  $90^{\circ}$ . More complex patterns result from overprinting of two or more fundamental systems. Bedrock jointing in lineament zones was analyzed in the Wartburg Basin area by Slusarski (1979) and Masuoka (1981) and was found to closely parallel lineament orientations. The same orientation relationship was found in this study. Lattman and Nickelson (1958) using lineaments detected on aerial photographs have extended bedrock joint mapping into areas covered by soil and trees.

Large structures on the Earth's surface due to their size and subtle expression, are often unrecognized in aerial photographic surveys. Seasat provides a synoptic view of the terrane which allows assessment of many larger structural features. These structures often correspond to known oil producing areas (Halbouty, 1976). The cost of an earth survey to establish a hydrocarbon resource target can be minimized using the regional approach provided by Seasat imagery.

## CHAPTER II

### THE RESEARCH AREA

#### I. GENERAL PHYSIOGRAPHIC SETTING

The Wartburg Basin covers an area of approximately 540 square miles (1400 sq km) and is centered at a point where Anderson, Scott, Morgan, and Campbell Counties come closest to a common corner. This area is part of the Cumberland Plateau section of the Appalachian Plateau Physiographic Province which trends northeastward across east-central Tennessee. The Cumberland Plateau is bounded by outward facing excarpments to the east and west and consists of several large, well defined areas, all with a general south-eastward dip of the Upper Paleozoic sediments.

The area is underlain by thick, clastic, nearly horizontal sedimentary rocks of Pennsylvanian Age. The eastern half of the Wartburg Basin is occupied by the Cumberland Mountains which are generally steep, with slopes averaging  $45^{\circ}$  and elevations varying from 840 feet (256m) to 3300 feet (1005m). The western half of the Wartburg Basin is covered by rolling hills with elevations varying from 820 feet (250m) to 1900 feet (579m).

## II. LOCATION OF THE STUDY AREA

The Wartburg Basin and surrounding area was recorded on revolution #852 as Seasat was moving in an ascending orbital node bearing  $N22.5^{\circ}W$  with a perpendicular look angle of  $N67.5^{\circ}E$  (Figure 2). The study area is located in the western quarter of the Wartburg Basin and the adjacent eastern edge of the Northern Cumberland Plateau Subprovince. This area, located in Scott and Morgan Counties, covers approximately 175 square miles (453 sq km) and lies within the Oneida South, Huntsville, Robbins, Rugby, Pilot Mountain, Gobey, Lancing, Camp Austin, and Petros 7.5 minute topographic quadrangles (Figure 3).

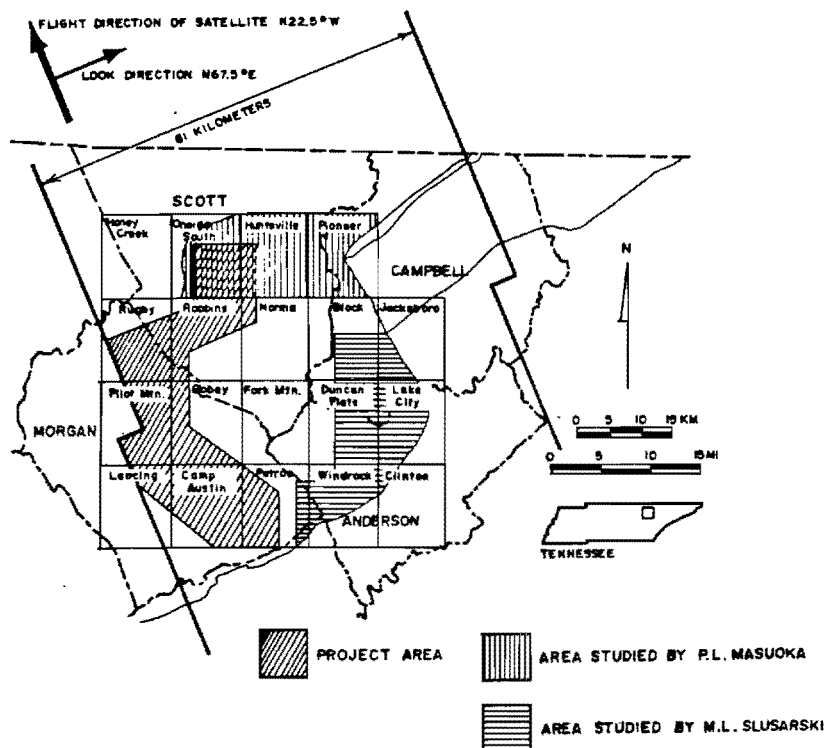


Figure 2. Location and extent of the project area covered by Seasat imagery.

## III. STRATIGRAPHY

Beds from nine regional groups of the Pennsylvanian Series form a thick mass of sedimentary rock up to 1200 feet (365m) thick in the study area. These consist mainly of interbedded shales and sandstones, siltstones, conglomerates, and minor amounts of coal (Luther, 1959). No rocks older than Pennsylvanian are exposed in the study area. The generalized stratigraphic column (Figure 4) proposed by Luther (1959) has been modified by Barlow (1969) who recommends that the lower boundary of the Cross Mountain

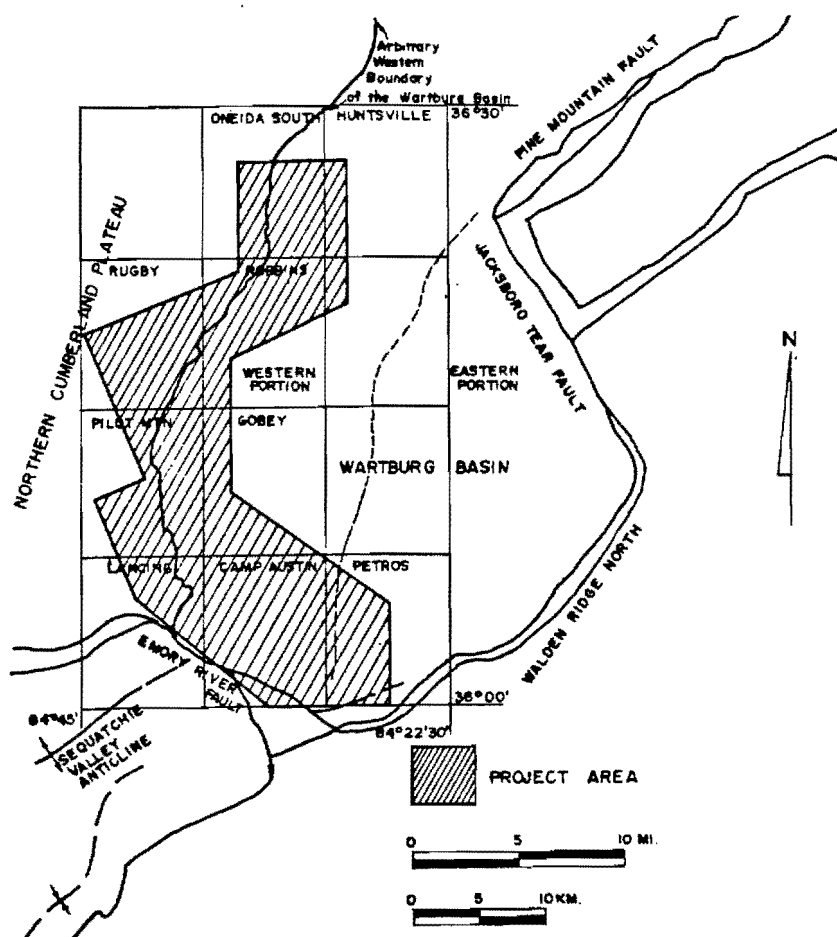


Figure 3. Location of the study area.

Group extend down to the Upper Pioneer Coal which takes in the Vowell Mountain Group, the Red Oak Mountain Group and the upper part of the Graves Gap Formation (Figure 5). The Cross Mountain Group, Graves Gap Formation, Indian Bluff Group, and Slatestone Group are found at higher elevations in the study area. No field stations occurred in these groups and formations. The majority of field stations occurred in the Crooked Fork Group, just below the Slatestone Group. Over 50% of the study area is overlain by the Crooked Fork Group.

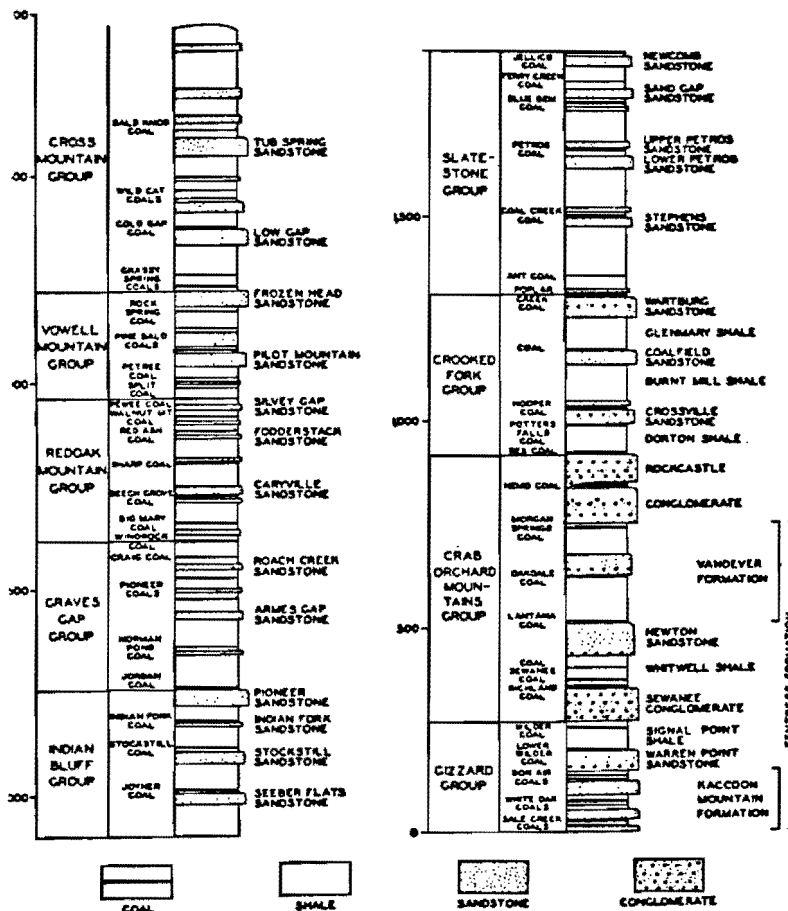


Figure 4. Generalized stratigraphic sequence of Pennsylvanian rocks in the Wartburg Basin area. (After Luther, 1959)

Keith, 1896	Glenn, 1925	Wanless, 1946	Wilson et al., 1956	Barlow, 1969		
ANDERSON SANDSTONE	ANDERSON FORMATION	ANDERSON FORMATION	CROSS MTN. GROUP	CROSS MOUNTAIN GROUP	CROSS MTN. FORMATION	ALLEGHENY
			Frozen Head Ss.		Rock Spring Coal	
SCOTT SHALE	SCOTT FORMATION	SCOTT FORMATION	VOWELL MTN. GROUP		CARYVILLE FORMATION	
			Pee wee Coal		Red Ash Coal	
			RED OAK MTN. GROUP		SASSAFRAS MTN. FORMATION	
			Windrock Coal		Up. Pioneer Coal	
			GRAVES GAP GROUP	GRAVES GAP FORMATION		
WARTBURG SANDSTONE	Pioneer Ss.	Pioneer Ss.	Pioneer Ss.	PIONEER SANDSTONE	POTTISVILLE (MANAWHA)	
JELICO FORMATION	JELICO FORMATION	INDIAN BLUFF GROUP				

Figure 5. Revisions in the nomenclature proposed by Barlow (1969).

#### IV. STRUCTURE

Five structural features influence the dip of Pennsylvanian rocks in the Wartburg Basin Area. From the west, beds dip gently into the Basin off the eastern flank of the Nashville Dome. To the northeast beds dip steeply into the Basin along the Pine Mountain and Jacksboro fault systems. Beds dip steeply into the Basin from the southeast along the edge of Walden Ridge North. To the southwest, beds dip gently into the Wartburg Basin off the Emory River fault and the Cumberland Plateau overthrust (Figure 6).



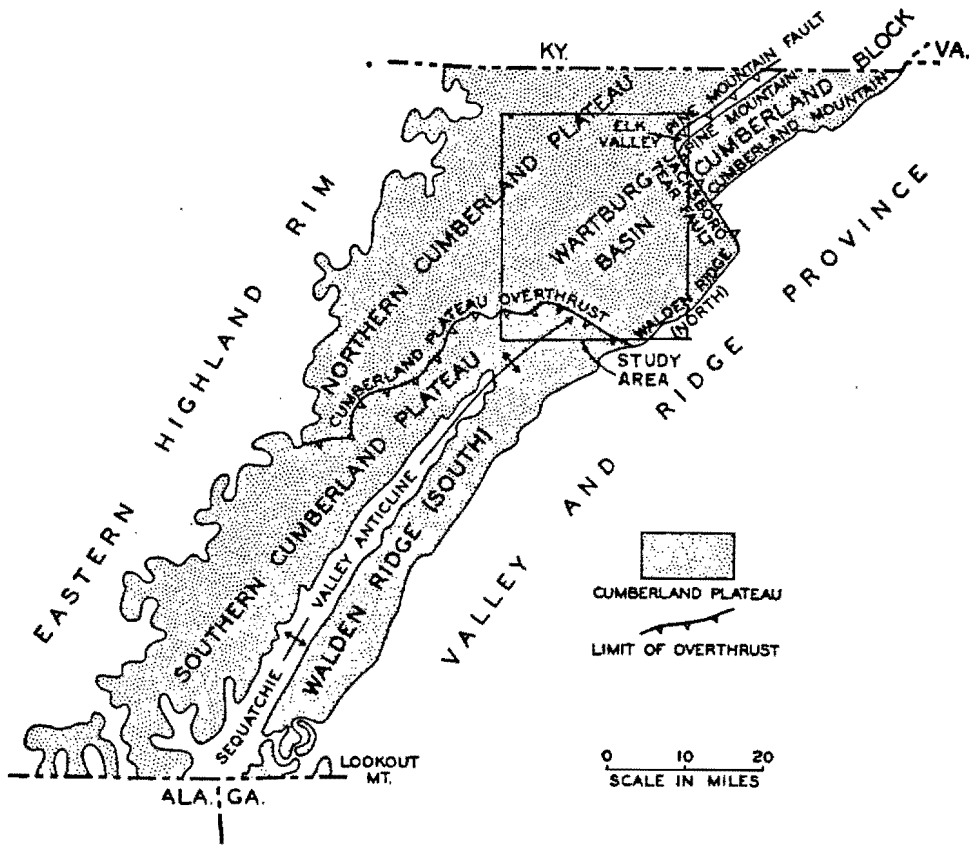


Figure 6. Structural features of the Wartburg Basin area. (After Luther, 1959)

## CHAPTER III

### INTERPRETING SEASAT IMAGERY

#### I. RADAR RETURN CHARACTERISTICS

Seasat imagery represents the amount of reflected microwave energy returning to the spaceborne antenna, the stronger the return, the brighter the image. Factors determining image brightness include surface physical properties, satellite orbital aberrations, man-made adjustments during orbit, and external atmospheric influences. A key factor in the amount of return signal intensity is the planar angle of the object sensed on the ground. Surface roughness also determines return signal intensity. Surfaces with an average vertical relief of 3.1 cm or less will appear smooth on the imagery and have a darker signature. Surfaces with a vertical relief of 5.7 cm or more will appear rough and have a brighter signature. Surfaces between these two values have intermediate values.

#### II. PICTURE ELEMENTS AND RESOLUTION

Four micropulses of the radar system within a 45 ft. to 164 ft. (13.7m to 50m) image footprint are averaged to form one picture element or pixel on Seasat imagery. Pixel resolution varies according to the type of image processing, either digital or optical correlation (NASA, 1980). Digitally correlated imagery has a higher resolution. Imagery

used in this analysis was optically correlated with a resolution of 98 ft. to 164 ft. (30m to 50m). To generate a single pixel from the raw product, thousands of computational operations are necessary using extremely fast and highly technical processing hardware. Resolution of Seasat imagery is limited mainly by distortion.

### III. DISTORTIONS

Seasat is a right-side looking radar system which illuminates a swath 62 miles wide (100km) extending 149 to 211 miles (240 to 340km) to the right of the subspacecraft point (Figure 7). With this imaging geometry, several types of common distortion are found on imagery of the Wartburg Basin. A layover distortion causes steep slopes to appear

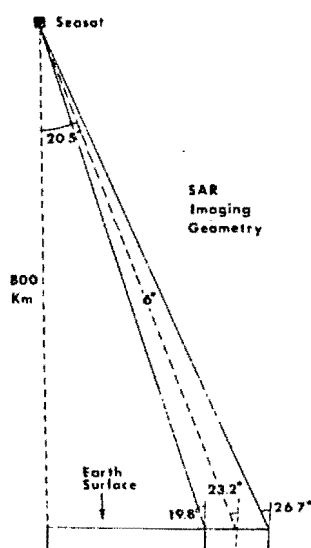


Figure 7. Seasat imaging geometry shown to scale in elevation view. (After Ford, 1980)

much steeper on the imagery. This occurs on imagery of the Cumberland Mountains in the eastern half of the study area. The upper part of the foreslopes, which are closer to the satellite in actual elevation, reflect the microwave signal before the pulse hits the lower part of the slopes (Figure 8). Foreshortening, which is similar to layover but not as pronounced, occurs on the imagery of the rolling hills in the western half of the study area. Radar shadowing occurs when backslopes facing away from the radar signal are steeper than the  $70^{\circ}$  look angle of the Seasat system. This occurs along steep, nearly vertical faces of outcrops and in a few of the strip-mined areas of the Wartburg Basin.

## DISTORTIONS:

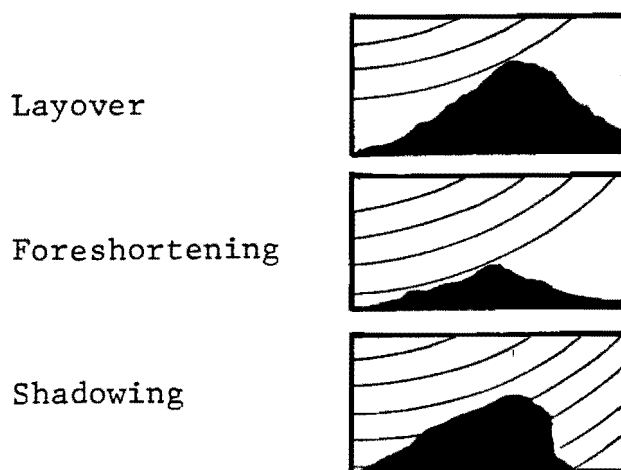


Figure 8. Common distortions on Seasat imagery.

Pixel elongation is another type of imagery distortion. Pixels in the study area are elongated approximately 2.5% in the look direction of the satellite (N67.5°E). The result is that for every 1000 feet (304.8m) of actual surface distance, the imagery is stretched out an additional 25 feet (7.6m). Adjustments had to be made during analysis to compensate for this inherent distortion.

Another limitation of Seasat which is not a distortion occurs when lineaments are parallel or subparallel (within plus or minus 15°) of the satellite look direction. They are often not detected when this situation occurs because the microwave pulse is reflected down the lineament trace and does not return to the orbiting antenna. This selective shadowing of lineaments is alleviated by a unique feature of Seasat coverage, opposed look directions. Many of the same areas were imaged by an ascending then a descending orbital node. Lineaments that fall within the 15° shadow zone of one node's look direction are often detected from the other node's look direction.

#### IV. LINEAMENTS ON THE IMAGERY

Image textures appear as stippled, granular areas ranging from fine to coarse grain. Image tones appear as smooth grey areas with up to six levels of intensity (Foster et al., 1981). Three basic types of lineaments can be defined on Seasat imagery (Figure 9). First, there are

lineaments that appear as long lines, either dark or light traces. Second, lineaments can appear as broader textural or tonal lines. Third, lineaments can appear as adjacent textural or tonal linear zones or bands. As lineaments are traced across varying topographic features, they often change from dark to light lines or change in texture, tone and even width.

A knowledge of weather conditions immediately before image acquisition is also important. Excessive rain significantly affects lineament enhancement and can cause more lineaments to appear on the imagery. Weather conditions were fair at the time of image acquisition in the study area.

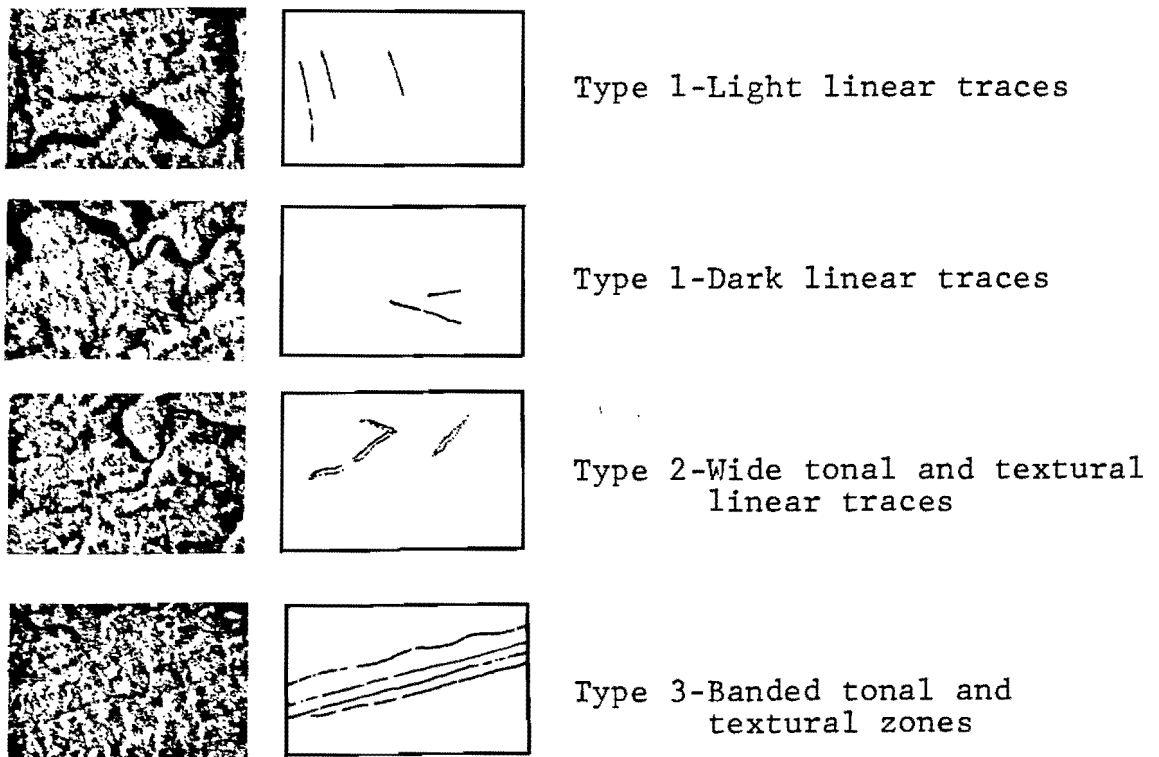


Figure 9. Examples of basic lineament types.

## V. ANALYSIS TECHNIQUES AND MATERIALS REQUIRED

Four 70 mm film strips represent one orbital pass of the satellite (NOAA, 1980). The filmstrip imagery was enlarged and printed at a scale of 1:250000, which corresponds with available geologic maps of the study area (Hardeman, 1966 and Watkins, 1964). Various acetate overlays were made from the geologic maps including major regional drainage patterns, mapped faults, cultural features, lithologies, and aeromagnetic and gravity contours. The overlays were applied individually and in combination to analyze Seasat imagery. Magnifications of the imagery ranged from 2X to 32X, but magnifications over 8X did not have the quality necessary for lineament analysis. 2X magnification, a scale of 1:125000, was used to map the majority of lineaments on the imagery. Extreme care must be taken when mapping at this scale, since a 0.1 inch (.254cm) error causes an approximate 1050 ft. (320m) map error.

One of the most notable features on Seasat imagery is the regional drainage system which is very detailed showing even small streams. By using the drainage overlay from the geologic map, pixel elongation could be corrected on the imagery. When the overlay was matched to drainage features on the imagery, surrounding lineaments were traced. Using this technique, 1186 tonal and textural linear features were mapped (Figure 10). This covers an

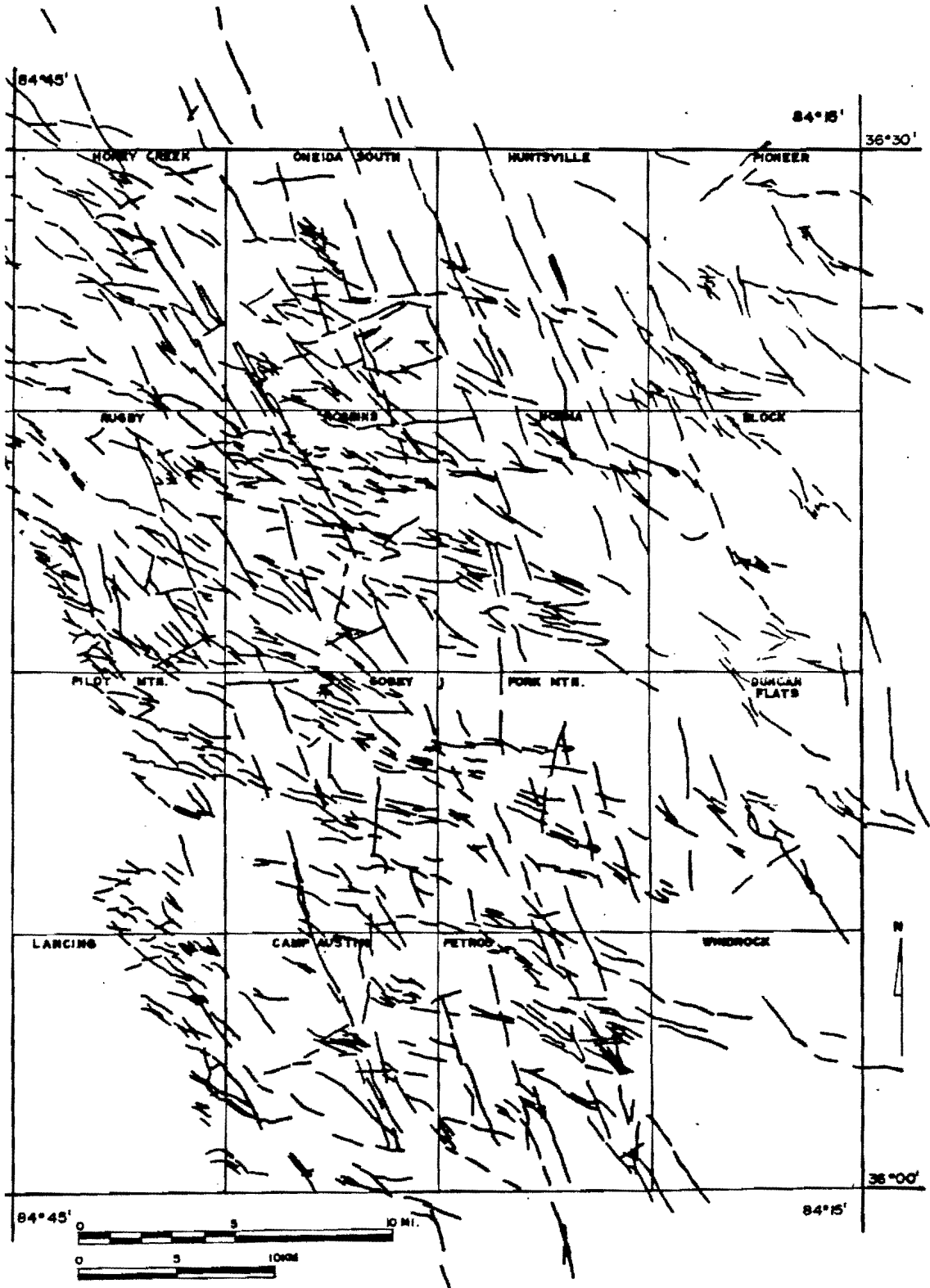


Figure 10. 1186 tonal and textural lineaments on Seasat imagery of the Wartburg Basin area.



area of approximately 900 square miles (2331 sq km) measuring approximately 28 miles by 38 miles (45km by 61km).

The general study area was analyzed five times. In order to map lineaments with maximum accuracy various techniques were used including directional changes in scanning the data, lighting angle changes, slight adjustments in magnification, alternate shifting of the imagery with the overlays, and the use of composite overlays. Once the final lineament maps were traced, they were applied to a 1:250000 geologic map and later enlarged and traced onto 7.5 minute USGS topographic quadrangles. The lineaments from the imagery were filtered on the quadrangles to eliminate all known man-made linear features. The aerial photographic imagery lineaments used in Slusarski and Masuoka's studies were also filtered to eliminate all known man-made linear features. Even with filtering approximately 10% of the lineaments found in the field were man-made. This situation is normal and does not significantly influence data analysis (Lattman et al., 1958).

## CHAPTER IV

### FIELD DATA ACQUISITION

#### I. LOCATING LINEAMENTS IN THE FIELD

Lineaments were easier to locate in man-made exposures such as strip-mine high walls, road cuts, railroad cuts, and large cultivated areas. Often longer lineaments were detected when they extended from inaccessible areas into more accessible areas. Of the 71 field stations chosen along projected lineaments (Figure 11), 43 stations (60%) had evidence of a lineament; 7 stations (10%) were either road segments, railroad segments, or power line right-of-ways; 21 field stations (30%) had no evidence of a lineament. Seven of the best field examples were selected to be shown in this study. The first four examples represent man-made exposures while the following three show the natural topographic expression of lineaments.

At each field station the following data were recorded:

1. Topographic orientation, depth and width of the lineament
2. Bedrock fracture orientations and dips in the lineament zone
3. Surrounding bedrock and topographic conditions, including drainage
4. Roadbed conditions when occurring in the zone
5. Oil or gas well production activity in the area.

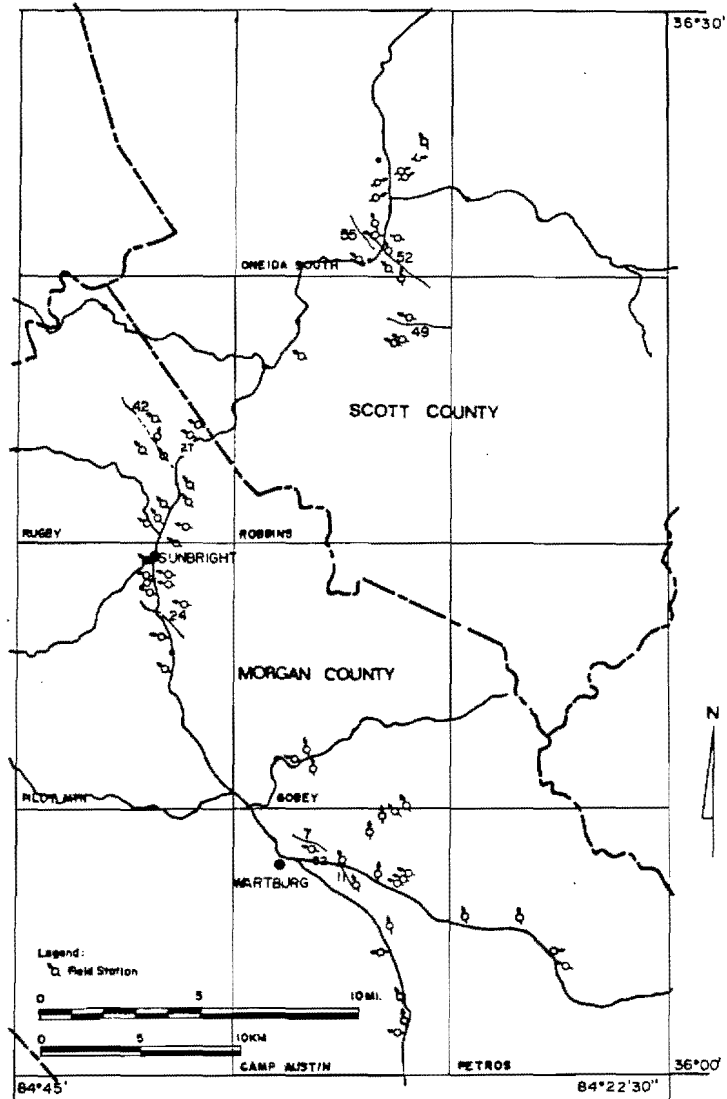


Figure 11. 71 field stations that were checked for lineaments. Field stations given as examples are numbered.

High vantage points were selected to study the general topography along lineament traces. If drainage was associated with a lineament, it was followed and observed. One of the main objectives in this study was to prove the accuracy of Seasat in locating lineaments. Initially, a 200 ft. (61m) margin of error to each side of the projected lineament was chosen; but lineaments occurring in bedrock exposures were usually within 50 feet (15m) of their projected map trace. Each example points out a different aspect about Seasat lineaments that was determined by field analysis.

Example 1: Field Station 49

Location: Strip-mine highwall, 1.75 miles (2.8km)  
northeast of Pleasant Mt. School, Robbins  
Quadrangle, Scott County.

Elevation: 1360 feet (414m) approximately

Lineament orientation: N84<sup>o</sup>W

Lineament length: 1.75 miles (2.8km)

Field station 49 is an example of a lineament with associated water seepage. Two parallel drainage rills were within 100 feet (30m) of Station 49. These two rills were dry and did not appear on the imagery. This lineament appears as a distinct, short, straight line on the imagery.

The interbedded sandstones and shales in the lineament zone are highly fractured (Figure 12). The bedrock is near-horizontal with a prominent diagonal fracture exposed in the upper portion of the highwall. The lineament

continues as a straight drainage indentation above the highwall and across Schoolhouse Ridge for approximately one mile (1.609km) to the southeast. The lineament continues down the hillside to the northwest as a straight, deeply incised stream segment.

Weather conditions are very important during image acquisition. If enough rain had fallen and collected in the surrounding drainage rills, they might have appeared on the imagery. Moisture in this type of lineament zone can cause a change in the dielectric constant which Seasat detects and enhances.



Figure 12. Field Station 49. Note the evidence of moisture in the lineament zone.

Example 2: Field Station 24

Location: Railroad cut, Southern Railway, 1.8 miles (2.9km) southeast of Sunbright, Tennessee, Pilot Mountain Quadrangle, Morgan County

Elevation: 1405 feet (428m) approximately

Lineament orientation: N61°W

Lineament length: 1.75 miles (2.8km) with one 300 ft. (91.4m) break at midpoint

Probable lineament locations are often verified by comparison with the surrounding terrane. A well defined, straight-line stream segment was the main evidence of the lineament in this example. This stream corresponds exactly with the proposed lineament from the imagery. When the surrounding area was examined no other straight stream segment could be found.

A small amount of bedrock is exposed in a railroad cut at Field Station 24 (figure 13). The crossbedded, flat-lying sandstone in the lower part of the exposure is not highly fractured. The thinbedded sandy shales overlying the sandstone are highly fractured but have no specific orientation. Most of the bedrock exposure along the lineament is obscured by thick stream deposits. The lineament continues approximately 250 feet (76m) from the Field Station to the southeast where it is obscured at midpoint by two road cuts. Although the lineament continues on the imagery to the northwest from the Field Station, no evidence of a topographic indentation could be found.





Figure 13. Field Station 24

Example 3: Field Station 55

Location: Railroad cut, Southern Railway, 0.5 mile (0.8km) north of New River, Tennessee, Oneida South Quadrangle, Scott County

Elevation: 1239 feet (377m)

Lineament orientation: N38°W

Lineament length: 3 miles (4.8km) with a 2000 ft. (609m) discontinuous portion at midpoint

The lineament at Field Station 55 appears on the imagery as a wide zone. In the field this lineament is made up of at least five parallel fractures, spaced 20 to 40 feet (6 to 12m) apart (Figure 14). These fractures dip 45° to the southwest and strike along the projected lineament. The adjacent hillside is also parallel to the fractures.



Figure 14. Parallel fractures at Field Station 55.

The interbedded sandstones and shales are highly fractured in the lineament zone (Figure 15). There is also a slight amount of normal faulting in the bedrock. The lineament becomes discontinuous on the imagery at the top of the hill above the outcrop at Station 55. Approximately 2000 feet (609m) to the southeast the lineament again appears on the imagery but no evidence of the trace could be found in the field. The imagery lineament resumes in an area of extensive oil and gas production. One well is located almost directly on the imagery trace. Hydrocarbon production in relation to lineament proximity is analyzed in Chapter VI.





Figure 15. Closer view of one of the fractures at Field Station 55. The scale equals one foot (30.48cm).

Examples 4 and 5: Field Station 52

Location: Road cut, 1000 feet (304m) from Highway 27,  
3500 feet (1066m) north of New River, Tenn.,  
Oneida South Quadrangle, Scott County

Elevation: 1420 feet (432m) approximate

Lineament orientation:  $N47^{\circ}W$

Lineament length: 2.5 miles (4km)

Two aspects of a lineament could be studied from this field station. Facing northwest, a roadcut exposes the lineament in the bedrock (Figure 16). Turning  $180^{\circ}$  to the southeast, the lineament appears as a subtle topographic

indentation which cuts a notch in Sheep Rock Mountain on the horizon (Figure 17).

The exposure to the northwest is made up of a thick, crossbedded sandstone in the lower section and thinner interbedded sandstones and siltstones in the upper section. The rocks in the upper section are highly fractured in the lineament zone while the thicker bedded sandstone in the lower section is fractured into larger blocks. The lineament extends to the northwest as a well defined, straight drainage rill. Although no active water seepage occurs



Figure 16. View to the northwest at Station 52. The scale equals one foot (30.48cm).

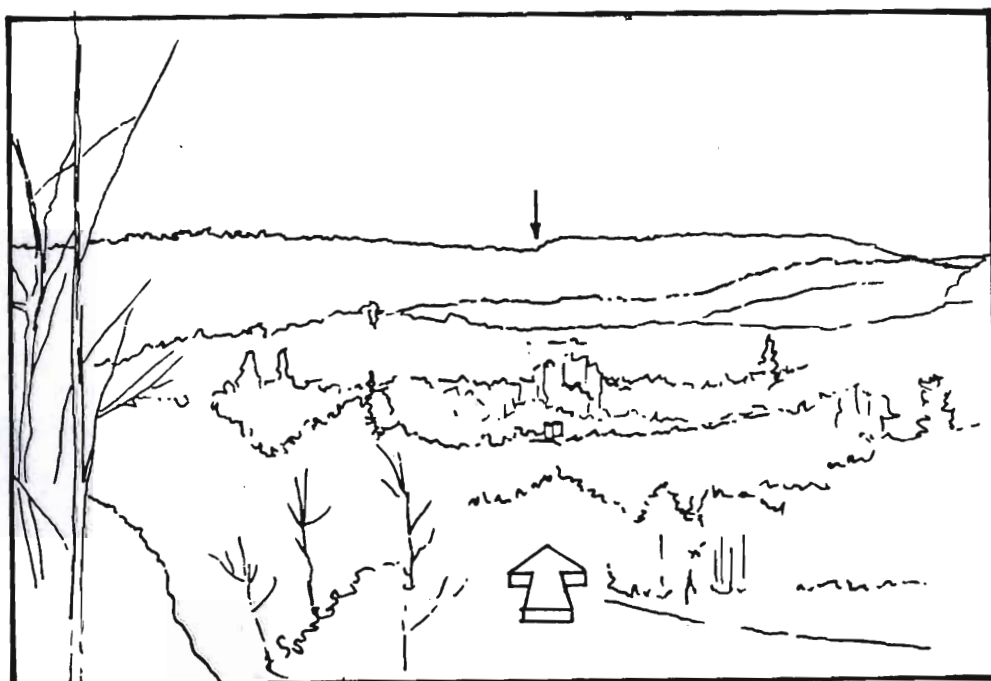


Figure 17. Example 5: Field Station 52. Photo and diagram of a projected lineament through an area with oil and gas production and across Sheep Rock Mountain.

at the exposure, a natural spring is located approximately 300 feet (91m) to the northwest along the lineament.

Facing southeast, the lineament extends for 1.75 miles (2.8km) crossing Sheep Rock Mountain on the horizon and continuing into Griffith Hollow approximately 0.5 mile (0.8km). The small notch in the ridge on the horizon corresponds exactly with the lineament trace on the imagery. This lineament is parallel to the lineament at Station 55 and is also located in an area of extensive oil and gas well production. Production of 308 wells in this area is analyzed in Chapter VI.

Example 6: Field Station 7

Location: 1.5 miles (2.4km) southeast of Wartburg,  
Tennessee, Camp Austin Quadrangle, Morgan  
County

Elevation: 1305 feet (397m) approximate

Lineament orientation:  $N73^{\circ}W$

Lineament length: 1.25 miles (2km), related to a  
swarm of subparallel lineaments

There are two basic types of lineaments in the study area, long lineaments which extend discontinuously for distances over 30 miles (48km), and short lineaments, usually 0.5 (0.8km) to 2 (3.2km) miles in length. The second type, shown in this example (Figure 18), occurs in tight groups or swarms of subparallel lineaments. Lineaments in these swarms often bifurcate or merge and they usually change orientations as a group. The lineament in



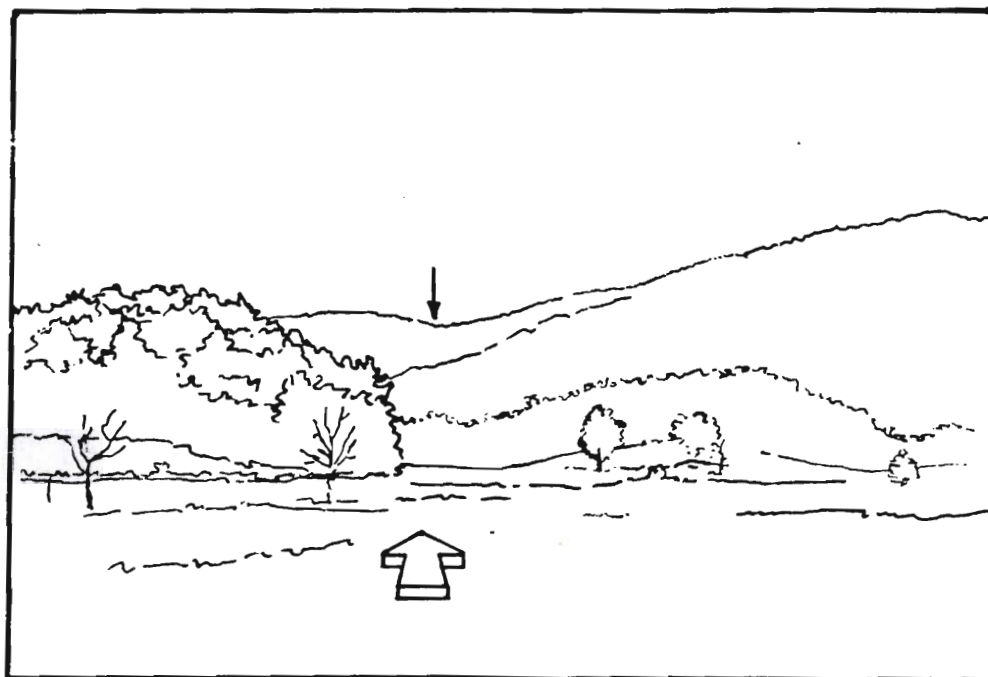


Figure 18. Example 6: Field Station 7. Photo and diagram of a lineament which crosses the valley floor and continues up the southeast slope of Bird Mountain.

Example 6 occurs as a small straight stream segment in the valley floor which continues up the slope of Bird Mountain. This stream cuts along the steep slope of a small hill in the valley floor. Surrounding hills were examined and no slopes were found to be steeply inclined. The lineament trace continues up the southeast slope of Bird Mountain and coincides with the center of an erosional gap on the crest of the ridge. The ridge area was studied extensively but no clear evidence of a lineament could be found. The lineament becomes discontinuous on the imagery on the northwest side of the ridge.

Example 7: Field Station 42

Location: Union Hill oil and gas field, 4.5 miles (7.2km) north of Sunbright, Tennessee, Rugby Quadrangle, Morgan County

Elevation: 1580 feet (481m)

Lineament orientation: N36.5°W

Lineament length: 4.25 miles (6.8km) with a discontinuous segment 2.25 miles (3.6km) long at midpoint

Example 7, which is situated on a discontinuous portion of the lineament, was chosen for two reasons. First, the field station occurs at a high vantage point from which evidence of the lineament can be seen to the northwest. Second, the effects of recent cultivation along the lineament zone can be observed. This station occurs between two perfectly aligned lineament traces on the imagery. Field observations show that when the lineament becomes

discontinuous on the imagery, both to the northwest and the southeast, a cultivated field begins. To the northwest the lineament begins in a forest beyond a cleared area and extends one mile (1.609km) across two small ridges (Figure 19). In the second ridge a distinct notch coincides with the lineament on the imagery. To the southeast approximately 3 miles (4.8km), a similar notch occurs along a ridgecrest which also coincides with the lineament on the imagery.

Extensive drilling activity has occurred in the lineament area. Three wells have been drilled within 100 feet (30m) of the projected discontinuous segment of the lineament in this example (Figure 20). These wells were analyzed for fracturing at depth in relation to lineament proximity. The results are discussed in Chapter VI.

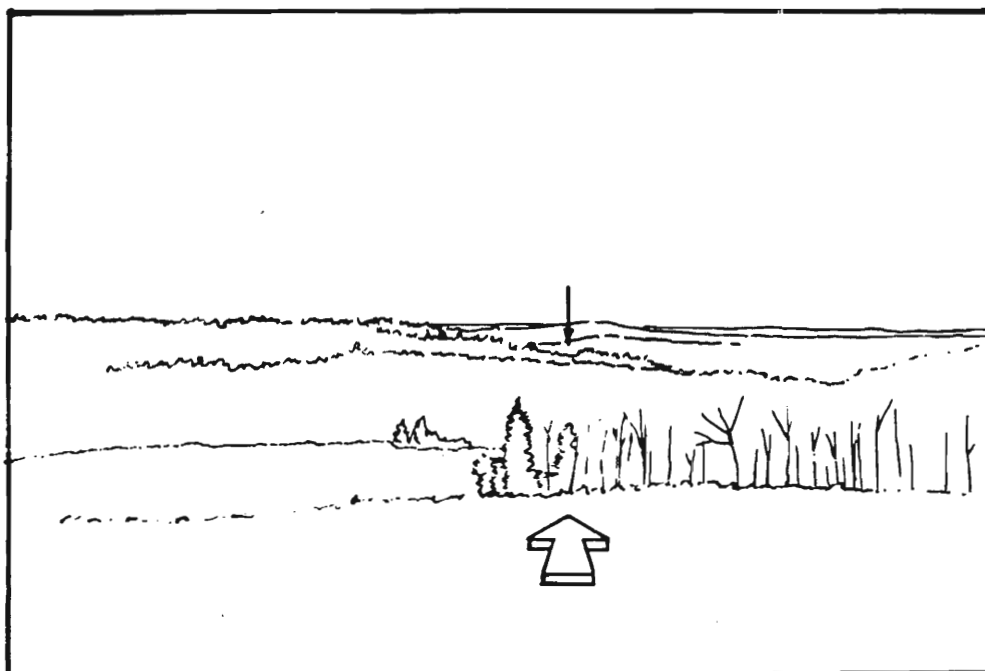


Figure 19. Example 7: Field Station 42. View to the northwest sighting along the lineament which appears on the imagery and coincides with a notch on the second ridge. The lineament becomes discontinuous as it enters the cultivated area in the foreground.





Figure 20. Drilling activity within 100 feet (30m) of the projected lineament in Example 7.

## CHAPTER V

### COMPARATIVE ANALYSIS OF LINEAMENTS IN THE STUDY AREA

#### I. SEASAT IMAGERY COMPARED TO AERIAL PHOTOGRAPHIC IMAGERY

One of the main objectives of this thesis is to compare Seasat lineaments to aerial photographic lineaments from the same area. Two other lineament studies have analyzed portions of the Wartburg Basin (Slusarski, 1979 and Masuoka, 1981). Lineaments from Masuoka's study area occur in the northeast corner of the Basin while Slusarski's lineaments are in the eastern edge of the Basin (Figure 2, page 8). These lineaments were compared to Seasat lineaments in the following categories:

1. Average lineament lengths comparison
2. Corresponding lineament segments
3. Probable lineament alignments
4. Crosscutting lineament terminations

#### Category 1: Average lineament lengths comparison

Average lineament lengths were compared to see if lineaments were longer on either type of imagery. A t-test (Morisawa, 1976) with a 0.05 level of significance (Guilford, 1956) was used in this category. Statistical analysis is based on the following data:

- N: Number of lineaments on each type of imagery
- X: Mean lineament lengths

Sum X: Sum of total lineament lengths

SD: Standard Deviation

t-crit: t value critical

t-cal: t value calculated

Null hypothesis: No significant difference exists between the average length of lineaments on Seasat imagery compared to the average length of lineaments on aerial photographic imagery.

Results: Based on the t-test, the null hypothesis was disproved. In Masuoka's area Seasat lineaments are longer, averaging 1.04 miles (1.67km) in length compared to lineaments 0.625 mile (1.0km) in length on aerial photographic imagery. Results are similar in Slusarski's area. Seasat lineaments average 1.305 miles (2.09km) compared to aerial photographic lineaments averaging 0.964 mile (1.55km) in length. Average lineament lengths on Seasat imagery by itself was also compared for the two areas. Using the t-test Seasat lineaments proved to be consistently longer in Slusarski's area. The same conclusion is true for aerial photographic lineaments in Slusarski's area. Table 1 presents the data from the statistical analysis.

Conclusions: Seasat may be able to detect even slight topographic indentations which are not as apparent on aerial photographic imagery. Moisture in lineament zones, even when the lineament is obscured, can also be detected by Seasat. This could extend beyond the visual observation of

TABLE 1: Comparison of Average Lineament Lengths on Seasat Imagery to Average Lineament Lengths on Aerial Photographic Imagery

	N Number of Lineaments	X Mean Lineament Length	Sum X Sum of Lineament Lengths	SD Standard Deviation	t-crit t value critical	t-cal t value calculated
Seasat Lineaments Masuoka Area	108	1.04 mi. (1.67km)	112.4mi. (180.8km)	0.6146	2.00	8.07
Aerial Photo Lineaments Masuoka Area	331	0.625 mi. (1.00km)	207 mi. (333km)	0.4018	2.00	
Seasat Lineaments Slusarski Area	56	1.305 mi. (2.09km)	73.1 mi. (117.6km)	0.7834	2.00	3.537
Aerial Photo Lineaments Slusarski Area	232	0.964 mi. (1.55km)	223.7 mi. (359.5km)	0.6077	2.00	

a lineament on the imagery. Often visual imagery requires shadowing, caused by a low sun angle, to reveal lineaments. Seasat requires no illumination source and is not limited by shadowing.

### Category 2: Corresponding Lineament Segments

One of the main purposes of this study is to see if Seasat imagery can detect the same lineaments as aerial photographic imagery. Lineaments or portions of lineaments which match from both types of imagery are shown as solid lines in Figure 21. Probable lineament alignments (Category 3) are shown as dotted lines. Comparative data for this category is presented in Table 2.

Results: The total length of lineaments from the combined imagery in Masuoka's area is 319.4 miles (513.9km).

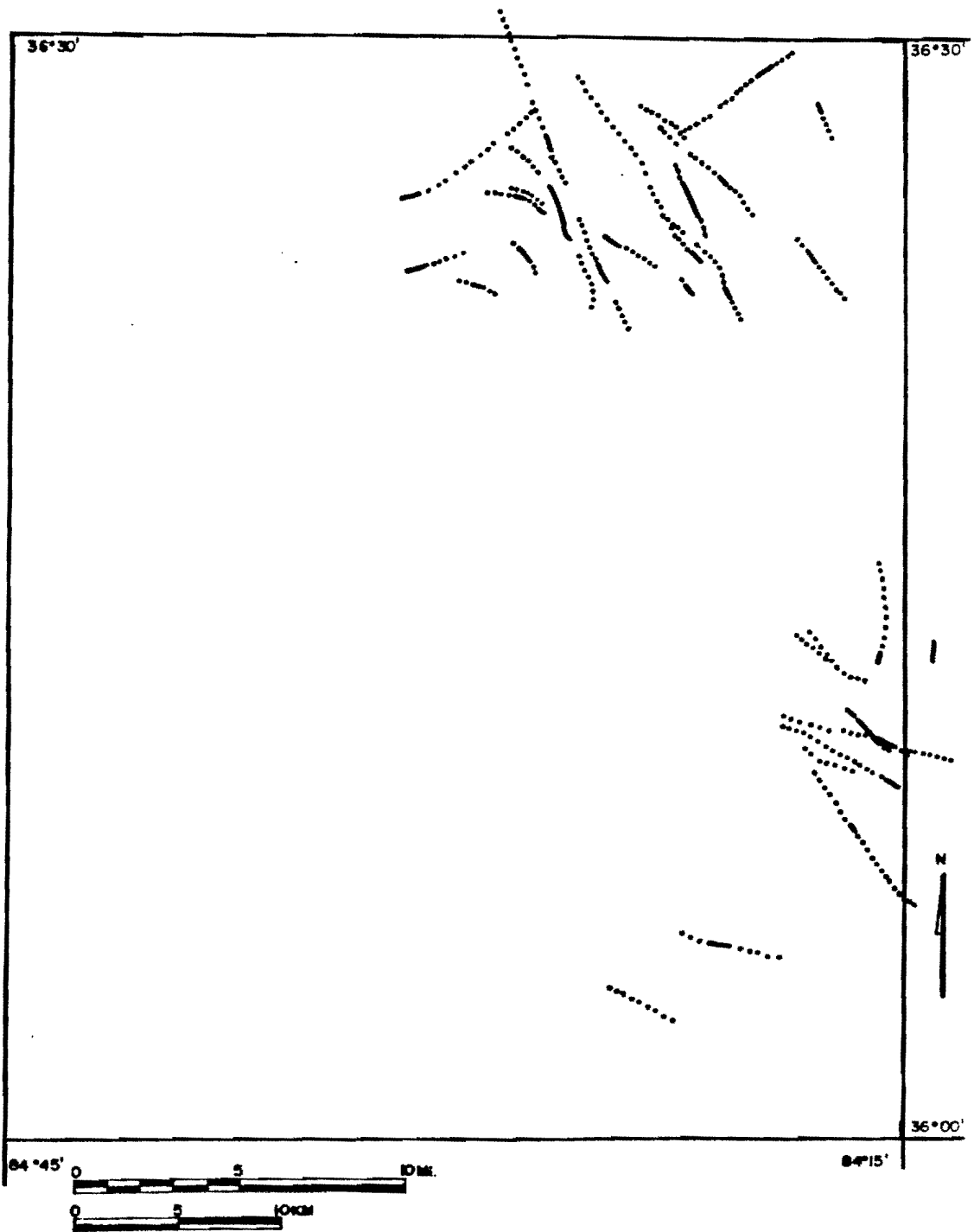


Figure 21. Matching lineaments (solid lines) from the combined imagery. Probable lineament alignments are shown as dotted lines.

TABLE 2: Comparison of the Number of Lineaments and Lineament Lengths from Seasat Imagery which Correspond to Lineaments on Aerial Photographic Imagery

	Seasat Lineaments	Aerial Photo Lineaments	Total	Corresponding Lineaments	Percentage of Total
Masuoka Area					
Number of Lineaments	108	331	439	17	3.8%
Lineament Lengths	112.4 mi. (180.8km)	207 mi. (333km)	319.4 mi. (513.9km)	9.4 mi. (15.1km)	2.94%
Slusarski Area					
Number of Lineaments	56	232	288	6	2.08%
Lineament Lengths	73.1 mi. (117.6km)	223.7 mi. (359.5km)	296.8 mi. (477.5km)	3.8 mi. (6.1km)	1.28%

17 lineaments in this area match, which represents 9.4 miles (15.1km), or 2.94%, of the total combined lineament lengths. In Slusarski's area combined total lineament lengths is 296.8 miles (477.5km). Only 3.8 miles (6.1km) of lineament lengths from the two types of imagery match in this area.

Conclusion: When this category is considered separately from Category 3, no significant correlation exists between lineaments on the two types of imagery.

### Category 3: Probable Lineament Alignments

Usually only small portions of lineaments from the two types of imagery matched in Category 2. Analysis shows that the discontinuous portion of a lineament from one type of imagery can be filled in by a lineament from the other type

of imagery. By using the combined imagery, probable, matching lineament lengths could be extended. The data is presented in Table 3.

Results: In Masuoka's area 41.2 miles (66.2km) of probable aligned lineament lengths were found. This is 12.9% of the total combined lineament lengths. In Slusarski's area 26.6 miles (42.7km) of probable aligned lineament lengths were found. This represents 8.9% of the total combined lineament lengths.

Conclusions: Combining Categories 2 and 3, 1.58 miles (2.54km) out of every 10 miles (16.09km) of lineament lengths in Masuoka's area are common to both Seasat and aerial photographic imagery. In Slusarski's area 1.02 miles (1.64) out of every 10 miles is common to both types of imagery. By combining Seasat imagery with aerial photographic imagery, discontinuous portions of lineaments can be filled in and lineament lengths extended.

TABLE 3: Comparison of Probable Lineaments and Lineament Lengths from Seasat Imagery which Correspond to Lineaments on Aerial Photographic Imagery

	Seasat Lineaments	Aerial Photo Lineaments	Total	Corresponding Lineaments	Percentage of Total
<b>Masuoka Area</b>					
Number of Lineaments	108	331	439	24	5.4%
Lineament Lengths	112.4 mi. (180.8km)	207 mi. (333km)	319.4 mi. (513.9km)	41.2 mi. (66.2km)	12.9%
<b>Slusarski Area</b>					
Number of Lineaments	56	232	288	12	4.1%
Lineament Lengths	73.1 mi. (117.6km)	223.7 mi. (359.5km)	296.8 mi. (477.5km)	26.6 mi. (42.7km)	8.9%

#### Category 4: Crosscutting lineament terminations

Often lineaments from one type of imagery are terminated by lineaments from the other type of imagery. This suggests a relationship between the lineaments. Possibly Seasat detects one type of lineament while aerial photographic imagery detects another. The data used in this study are presented in Table 4. The terminations are shown in Figure 22.

Results: Crosscutting terminations were first considered for each type of imagery then for the combined imagery. An additional 89 terminations were observed in Masuoka's area when the two types of imagery were combined. The results are similar in Slusarski's area. 41 additional terminations (14.2%) resulted from the combined imagery.

Conclusions: When a lineament becomes discontinuous on either type of imagery in Masuoka's area, in one out of every five cases, the lineament was stopped by a crosscutting lineament from the other type of imagery. In Slusarski's area, one out of every seven lineaments on either type of imagery is stopped in this manner. One type of imagery can be used to explain why a lineament stops on the other type of imagery.

Figure 23 shows the aerial photographic lineaments (darker lines) compared to Seasat lineaments (lighter lines). Masuoka's lineaments are in the upper portion of the figure. Slusarski's lineaments are in the lower right section.



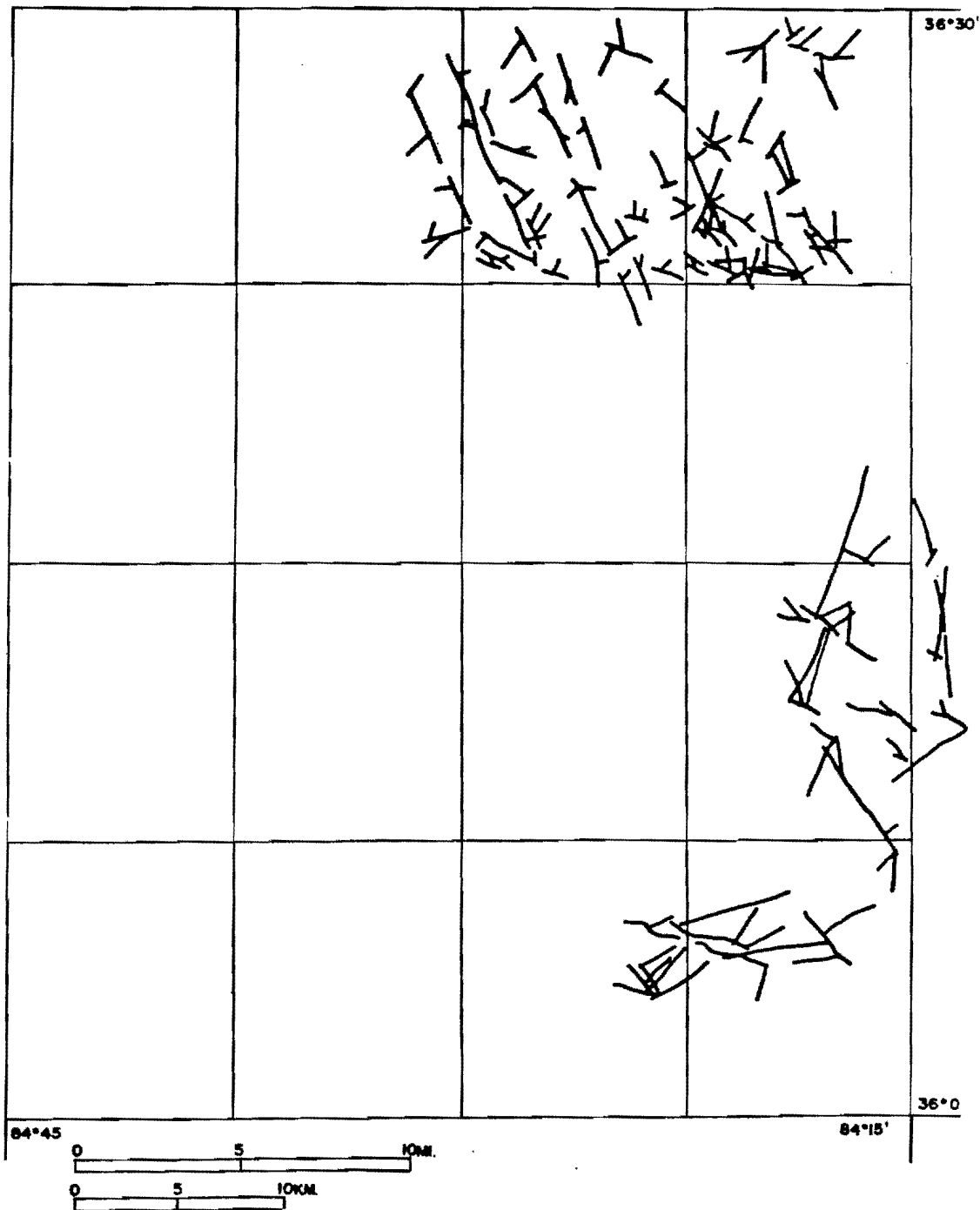


Figure 22. Lineaments terminated by crosscutting lineaments from the combined imagery.

TABLE 4: Seasat Lineament Terminations Compared to Aerial  
Photographic Lineament Terminations

	Number of Lineaments	Number of Terminations	Percentage of Terminations
<b>Masuoka Area</b>			
Seasat Lineaments	108	18	16.6%
Aerial Photo Lineaments	331	116	35%
Combined Imagery Lineaments	439	89	20.2%
<b>Slusarski Area</b>			
Seasat Lineaments	56	14	25%
Aerial Photo Lineaments	232	96	41.4%
Combined Imagery Lineaments	288	41	14.2%

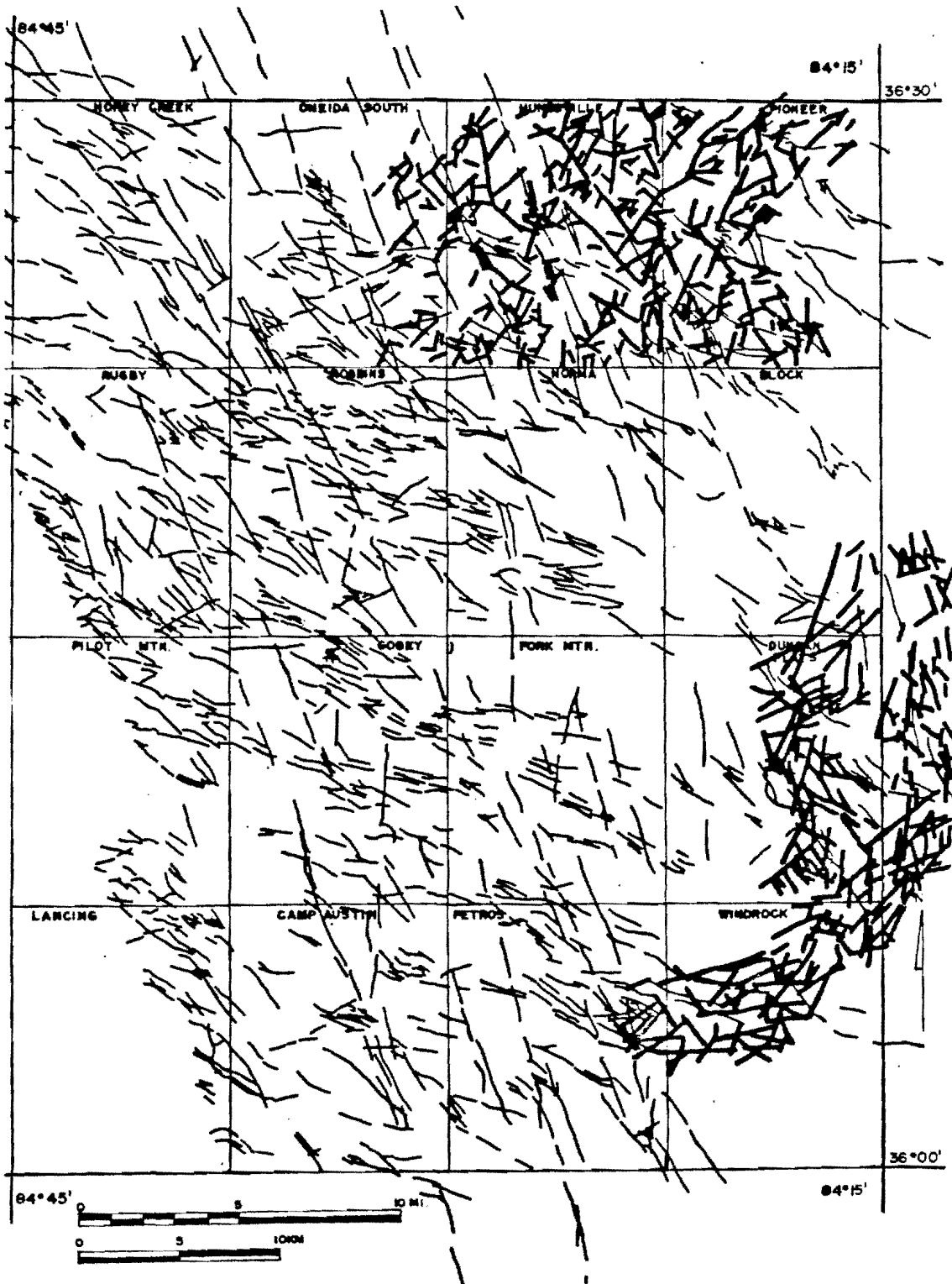


Figure 23. Aerial photographic lineaments (darker lines) compared to Seasat lineaments.

## II. GENERAL STUDY AREA ANALYSIS: FOUR LINEAMENT SYSTEMS

The methods used to analyze lineaments in Masuoka and Slusarski's areas were also applied to lineaments in the general study area. Lineaments traced from the Seasat imagery were arbitrarily broken into four systems based on orientation (Table 5)

TABLE 5: Breakdown of 1186 Lineaments into Four Systems

System	Orientation	Number of Lineaments per System
1	0°N to N35°W	203
2	N35°W to N65°W	504
3	N65°W to N90°W	381
4	0°N to N90°E	98

Figure 24 shows the four systems in a rose diagram and also the radar shadow zone which limits the number of lineaments occurring in System 4.

The following categories were chosen for comparative analysis of the four systems:

1. Average lineament lengths
2. Lineaments parallel to drainage with respect to distance

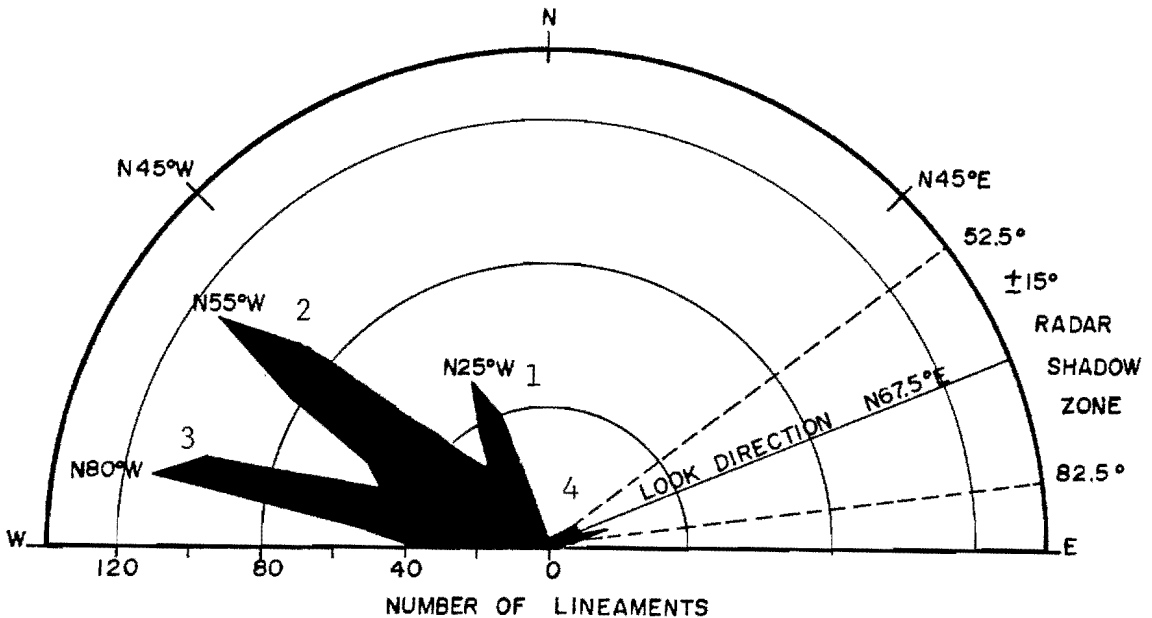


Figure 24. Rose diagram of the four lineament systems.

3. Lineaments terminated by drainage
4. Crosscutting lineament terminations
5. Lineaments related to gravity contours
6. Lineaments related to aeromagnetic contours.

Category 1: Average lineament lengths

A comparison of average lineament lengths in the four systems was made using the t-test (Morisawa, 1976) with a 0.05 level of significance (Guilford, 1956). Statistical analysis was based on the following data:

- N: Number of lineaments per system
- X: Average lineament lengths
- Sum X: Total lineament lengths
- SD: Standard Deviation
- t-crit: t value critical

t-cal: t value calculated

Null hypothesis: There is no significant difference between the average lineament lengths in System 1 compared to the average lineament lengths in Systems 2, 3, and 4.

Results: Based on the calculated values shown in Table 6, the null hypothesis was rejected. The average length of lineaments in System 1, 1.39 miles (2.23km), is longer than average lengths in Systems 2, 3, and 4. The same type of null hypothesis was used to compare each system to the other three. System 4 was found to differ significantly from the other systems. System 2 was not significantly different from System 3.

Conclusions: Based on this analysis, Systems 2 and 3 could possibly be combined into one system. Lineaments in System 1 are significantly longer than the other systems. Figure 25 shows the four lineament systems. At least 6 major lineaments over 35 miles (56.3km) in length occur in System 1. These longer lineaments are broken apart by short discontinuous segments. In other areas, longer lineaments have been related to basement penetrating fracture zones (Smith and Drahovzal, 1972). Lineaments in Systems 2 and 3 appear to be similar in length and grouping.

Category 2: Lineaments parallel to drainage with respect to distance

Lineaments up to one mile (1.609km) from major streams and rivers were considered in this category. The Chi square

TABLE 6: Comparison of Average Lineament Lengths in the Four Systems

System	N Number of Lineaments	X Mean Lineament Length	Sum X Sum of Lineament Lengths	SD Standard Deviation	t-crit t value critical	t-cal t value calculated
1	203	1.39 mi. (2.23km)	282.1 mi. (453.8km)	0.7272		
2	504	0.786 mi. (1.26km)	396.2 mi. (637.4km)	0.4376	2.00	13.520
3	381	0.744 mi. (1.19km)	283.5 mi. (456km)	0.4359	2.00	13.359
4	98	0.922 mi. (1.48km)	90.4 mi. (145.4km)	0.9007	2.00	4.830

test (Ambrose et al., 1977) with a 0.05 level of significance (Steel et al., 1960) was used for this category and Categories 3 thru 6. This test was used to compare each system to a norm. Data are presented in Table 7.

N: Number of lineaments per system

n: Number of lineaments per 100 ft. (30.4m) increment

$n/N(100)$ : Percentage per increment

$n/N(100)_{exp}$ : Expected Percentage per increment

cv: Critical value

cv-cal: Calculated critical value

Null hypothesis: The observed number of lineaments parallel to drainage equals the expected number of lineaments parallel to drainage.

Results: The null hypothesis was rejected by System 1 in the 0.0 to 0.25 mile (0.4km) interval. This was the only system and the only interval which had a significantly

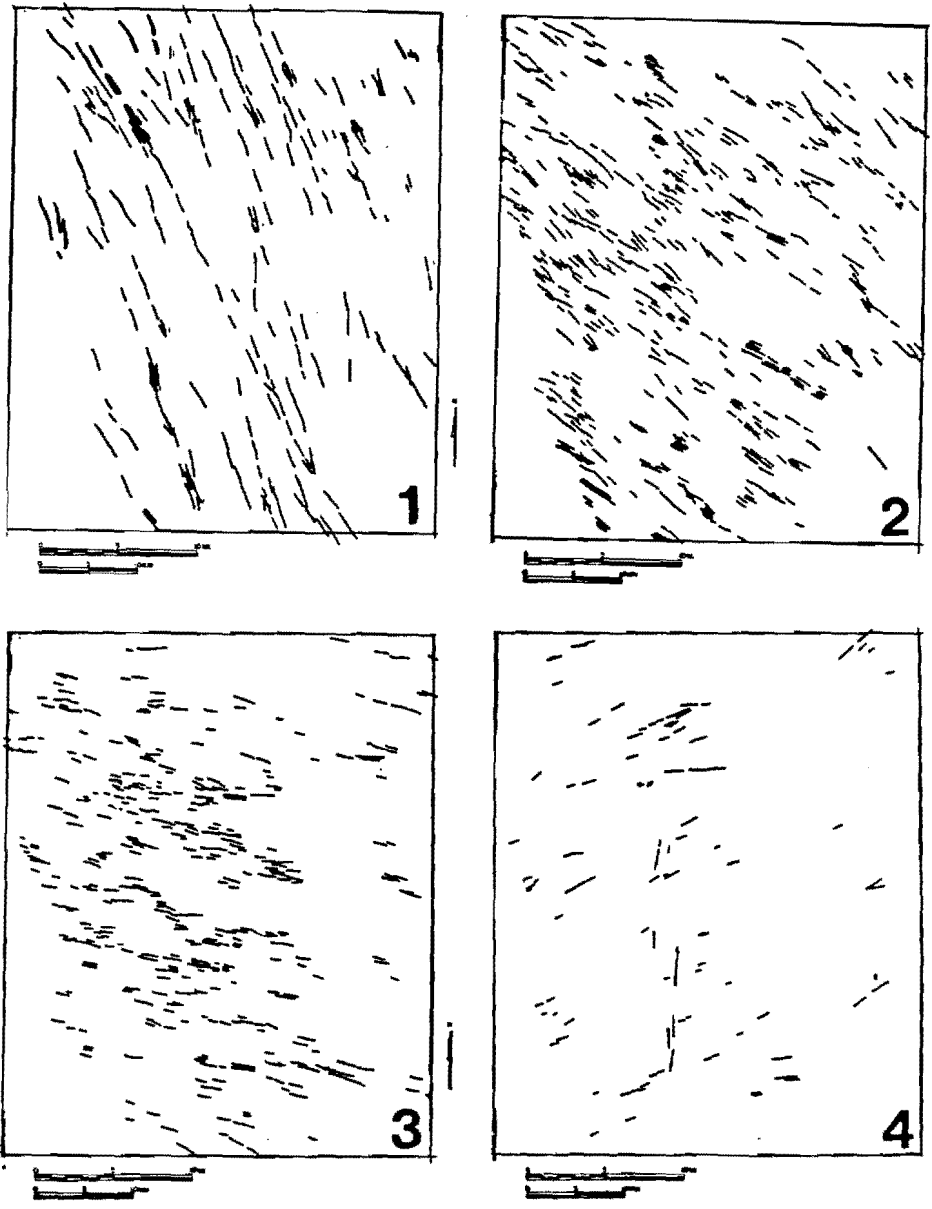


Figure 25. The four lineament systems in the general study area.



greater number of lineaments parallel to drainage. 41% of all lineaments in System 1 are parallel to drainage, compared to the expected norm of 29%. The other three systems do not differ significantly from the norm.

Conclusions: Based on this analysis, approximately one out of every four lineaments in System 1 is closely related to major drainage in the study area.

Category 3: Lineaments terminated by drainage

When the drainage network overlay was applied to the lineament overlay, a number of lineaments were observed to be terminated by drainage (Figure 26). Drainage may significantly influence one or more of the lineament systems. A statistical analysis was based on the following data (Table 8):

N: Number of lineaments per system

n: Number of lineaments terminated by drainage

$n/N(100)$ : Percentage of terminations per system

$n/N(100)_{exp}$ : Expected percentage of terminations

cv: Critical value

cv-cal: Calculated critical value

Null hypothesis: The observed number of lineaments terminated by drainage equals the expected number of lineaments terminated by drainage.

Results: Based on statistical evidence, System 1, with 30.5% drainage related terminations, differed significantly from the norm of 18.8% terminations. System 1, when compared

TABLE 7: Comparison of Lineaments Parallel to Drainage with Respect to Distance

System and Increment	N Number of Lineaments per System	n Number of Lineaments per Increment	n/N(100) Percentage per Increment	n/N(100)exp Expected Percentage per Increment	cv critical value	cv-cal calculated critical value
System 1	203					
0.0 to 0.25 mi.		44	22%	13%	3.84	6.23
0.25 to 0.50 mi.		19	9%	9%	3.84	0.11
0.50 to 0.75 mi.		10	5%	4%	3.84	0.25
0.75 to 1.00 mi.		<u>10</u>	<u>5%</u>	<u>3%</u>	3.84	0.66
		83 total	41% total	29% total		
System 2	504					
0.0 to 0.25 mi.		52	10%	13%	3.84	3.00
0.25 to 0.50 mi.		39	8%	9%	3.84	1.00
0.50 to 0.75 mi.		19	4%	4%	3.84	0.00
0.75 to 1.00 mi.		<u>15</u>	<u>3%</u>	<u>3%</u>	3.84	0.00
		125 total	25% total	29% total		
System 3	381					
0.0 to 0.25 mi.		42	11%	13%	3.84	2.00
0.25 to 0.50 mi.		41	11%	9%	3.84	2.00
0.50 to 0.75 mi.		12	3%	4%	3.84	1.00
0.75 to 1.00 mi.		<u>8</u>	<u>2%</u>	<u>3%</u>	3.84	1.00
		103 total	27% total	29% total		
System 4	98					
0.0 to 0.25 mi.		13	13%	13%	3.84	0.00
0.25 to 0.50 mi.		10	10%	9%	3.84	1.00
0.50 to 0.75 mi.		3	3%	4%	3.84	1.00
0.75 to 1.00 mi.		<u>1</u>	<u>1%</u>	<u>3%</u>	3.84	2.00
		27 total	27% total	29% total		

TABLE 8: Comparison of Lineaments Terminated by Drainage

System	N Number of Lineaments per System	n Lineaments Terminated	n/N(100) Percentage of Terminations	n/N(100)exp Expected Percentage of Terminations	cv critical value	cv-cal calculated critical value
1	203	62	30.5%	18.8%	3.84	7.28
2	504	99	19.6%	18.8%	3.84	0.034
3	381	42	11.0%	18.8%	3.84	3.23
4	98	21	21.4%	18.8%	3.84	0.35

statistically to the other 3 systems, also differed significantly. The other three systems remained within the norm.

Conclusions: Lineaments in System 1 are highly influenced by major drainage. This could indicate that stream dissection formed after the longer lineaments in System 1 were established.

Category 4: Crosscutting lineament terminations

Two types of crosscutting relationships occur. A lineament is either terminated by another lineament or it terminates another lineament. These two relationships are readily seen on Figure 27. This category does not distinguish between the two types of termination. Statistical analysis is based on the following data (Table 9):

N: Number of lineaments per system

n: Number of lineaments per system involved in terminations

n/N(100): Percentage of terminations

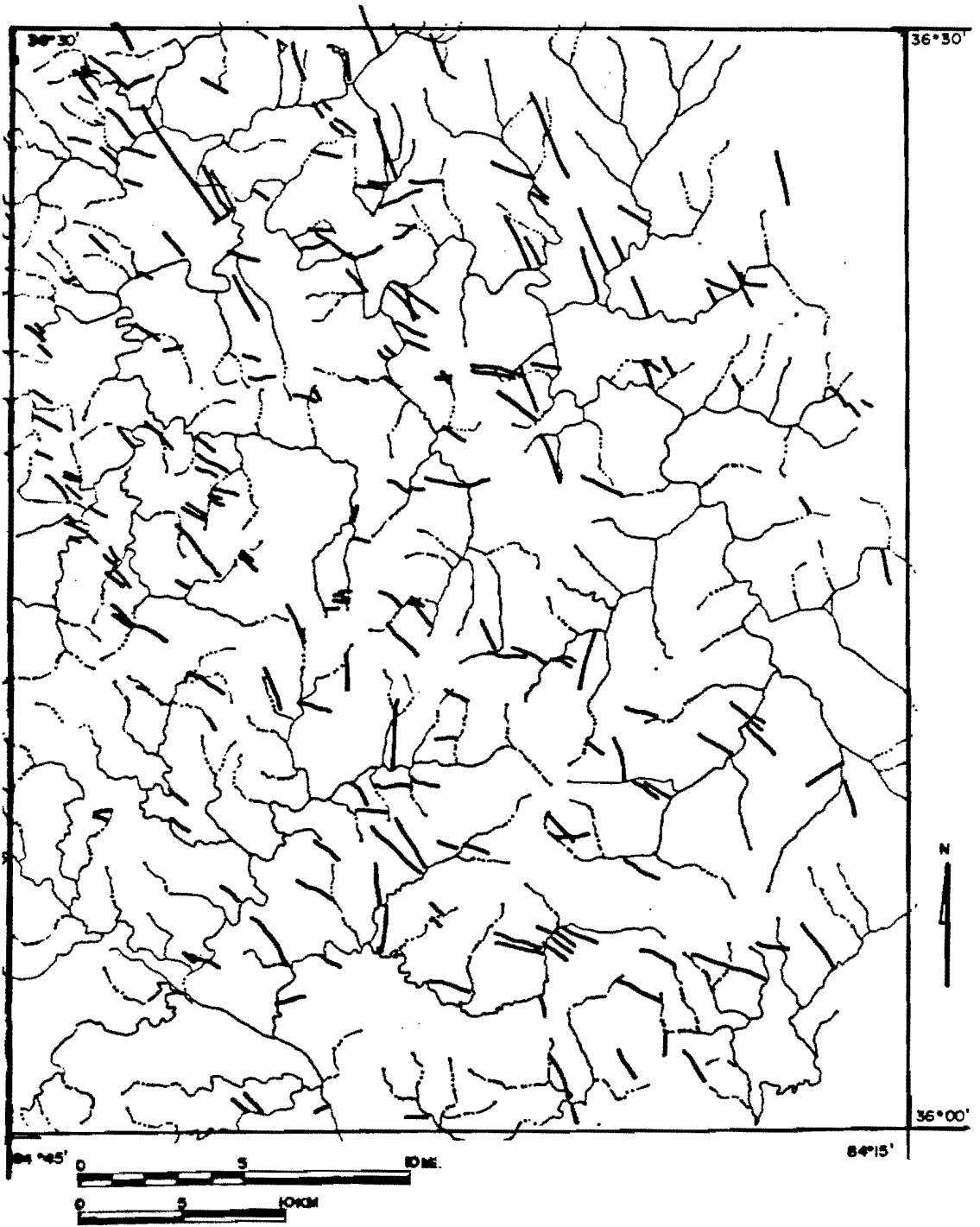


Figure 26. Lineaments terminated by drainage.

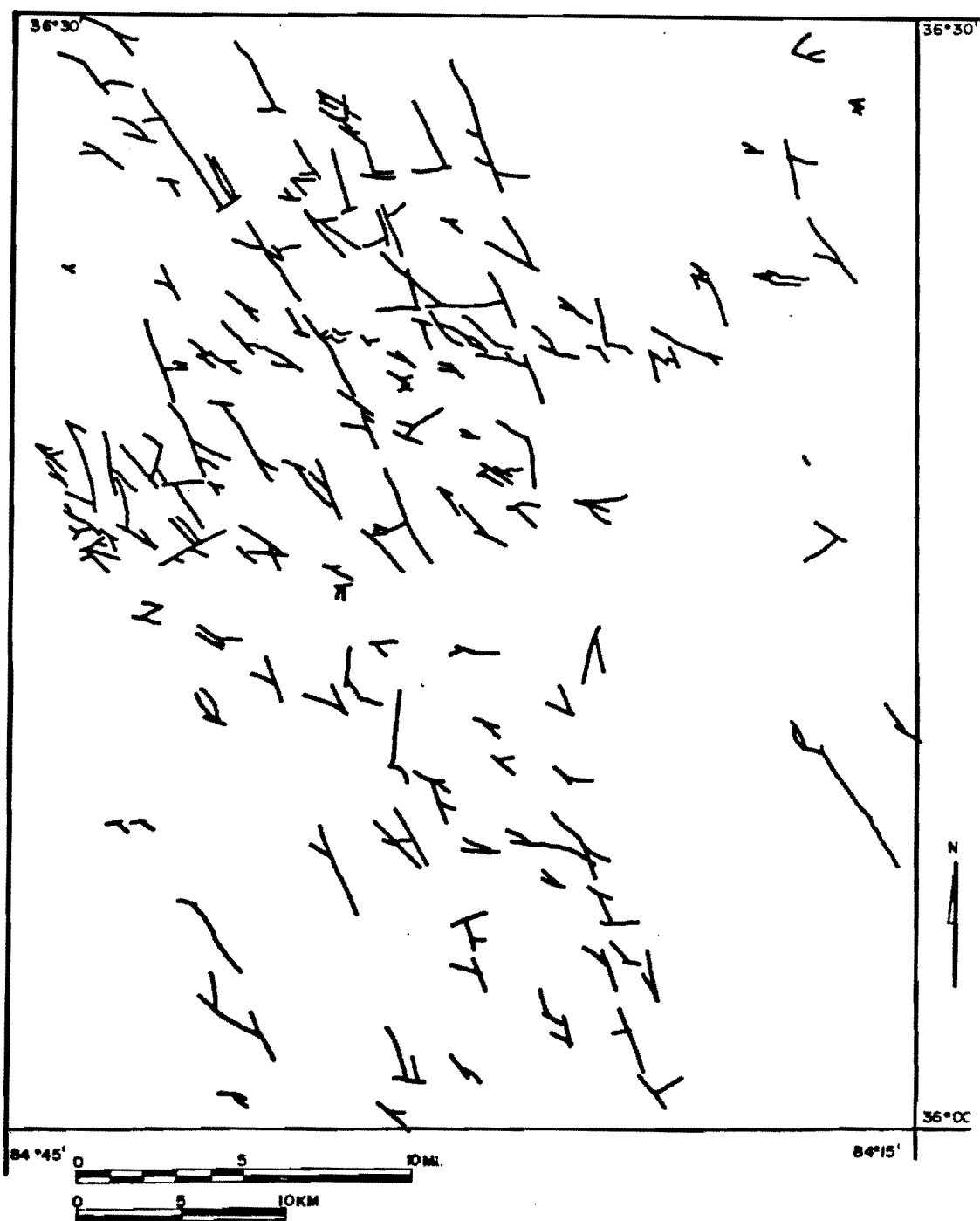


Figure 27. Lineaments terminated by crosscutting lineaments.

$n/N(100)_{exp}$ : Expected percentage of terminations

cv: Critical value

cv-cal: Calculated critical value

Null hypothesis: The observed number of lineaments involved in crosscutting terminations equals the expected number of lineaments involved in terminations.

Results: The null hypothesis was rejected by Systems 1 and 4. 40.8% of all lineaments in System 1 and 42.8% of all lineaments in System 4 are involved in crosscutting terminations. Systems 2 and 3 did not differ significantly from the norm.

Conclusions: The relationships between crosscutting lineaments is not well understood. Possibly a sequence of structural events is involved. Another statistical analysis was made to determine whether one of the systems caused more lineament terminations. No one system was responsible for a significantly greater number of terminations.

TABLE 9: Comparison of Lineaments Terminated by other Lineaments

System	N Number of Lineaments per System	n Lineaments Terminated	$n/N(100)$ Percentage of Terminations	$n/N(100)_{exp}$ Expected Percentage of Terminations	cv critical value	cv-cal calculated critical value
1	203	83	40.8%	27.3%	3.84	6.25
2	504	125	24.4%	27.3%	3.84	0.33
3	381	74	19.4%	27.3%	3.84	2.10
4	98	42	42.8%	27.3%	3.84	8.33

Category 5: Lineaments related to gravity contours

Lineaments can reflect basement trends (Dobrin, 1976) which in turn are reflected in gravity contours (Watkins, 1964). Although this thesis does not attempt to structurally interpret basement conditions in the Wartburg Basin, relationships were found between lineament trends and gravity contours. The Bouguer gravity values in the study area vary a total of 50 mgal with regional gravity gradients generally sloping southeast. In the area between the Emory and Jacksboro Faults, there is a pronounced gravity anomaly, due either to increased basement elevation or changes in basement lithologies (Watkins, 1964). The lineaments which are parallel or subparallel to gravity contours are shown in Figure 28. Statistical analysis was made to determine any relationships between the lineament systems and gravity trends. Analysis is based on the following data which is presented in Table 10:

N: Number of lineaments per system

n: Number of lineaments related to gravity contours

$n/N(100)$ : Percentage of related lineaments

$n/N(100)_{exp}$ : Expected percentage of lineaments

cv: Critical value

cv-cal: Calculated critical value

Null hypothesis: The observed number of lineaments parallel or subparallel to gravity contours in any one system is equal to the expected number of lineaments parallel or subparallel to gravity contours.

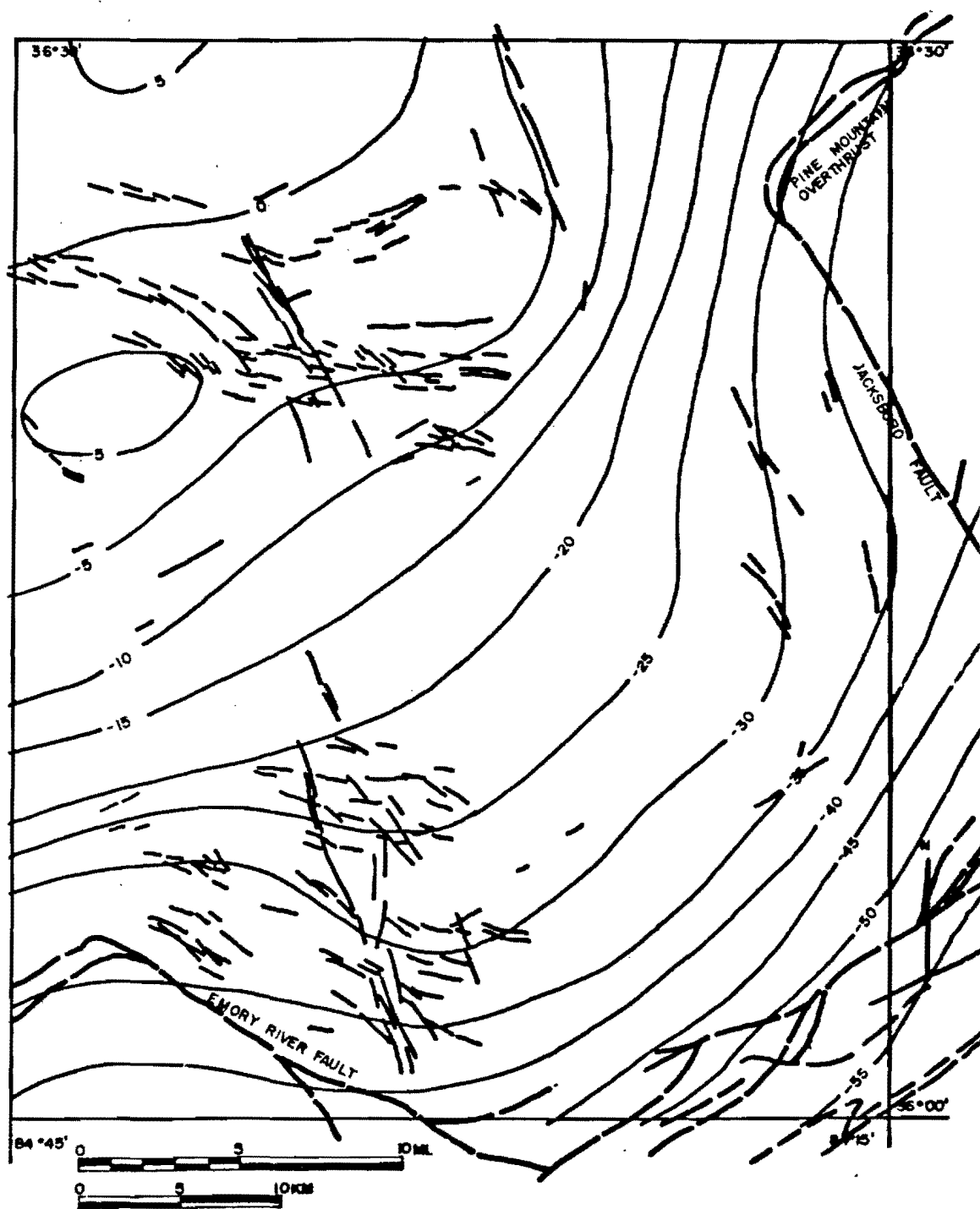


Figure 28. Lineaments related to gravity contours.



Results: The null hypothesis was rejected by System 4. 34.6% of all lineaments in this system are aligned with gravity contours. Systems 1, 2, and 3 do not differ significantly from the norm.

Conclusions: The lineaments in System 4 coincide with the general northeast to southwest trend of the gravity isogals. This could indicate that the lineaments in System 4 are reflecting basement-related fractures that trend with the gravity contours.

TABLE 10: Comparison of Lineaments Aligned with Gravity Contours

System	N Number of Lineaments per System	n Aligned Lineaments	n/N(100) Percentage of Lineament Alignments	n/N(100)exp Expected Percentage of Lineament Alignments	cv critical value	cv-cal calculated critical value
1	203	46	22.6%	19.4%	3.84	0.52
2	504	77	15.6%	19.4%	3.84	0.74
3	381	72	18.8%	19.4%	3.84	0.01
4	98	34	34.6%	19.4%	3.84	10.9

Category 6: Lineaments related to aeromagnetic contours

Magnetic contours in the Wartburg Basin are the result of variations in the susceptibility of the Precambrian basement (Watkins, 1962). Almost twice as many lineaments are related to aeromagnetic trends than to gravity trends. A statistical analysis based on the following data was made to determine any significant relationship (Table 11):

N: Number of lineaments per system

n: Number of lineaments related to aeromagnetic contours

$n/N(100)$ : Percentage of related lineaments

$n/N(100)_{exp}$ : Expected percentage of related lineaments

cv: Critical value

cv-cal: Calculated critical value

Null Hypothesis: The observed number of lineaments in each system which align with aeromagnetic trends equals the expected number of lineaments that are aligned with aeromagnetic trends.

Results: The null hypothesis was not rejected by any of the systems.

Conclusions: No particular system shows a close relationship to aeromagnetic contours (Figure 29). When the four systems are combined, they form groups or swarms of lineaments that trend with the contours. The aeromagnetic lineament overlay was also applied to the gravity lineament overlay. From the combined total of 685 lineaments, 84 lineaments, or 12.5%, were common to both aeromagnetic and gravity contours.

TABLE 11: Comparison of Lineaments Related to Aeromagnetic Contours

System	N Number of Lineaments per System	n Related Lineaments	$n/N(100)$ Percentage of Related Lineaments	$n/N(100)_{exp}$ Expected Percentage of Related Lineaments	cv critical value	cv-cal calculated critical value
1	203	83	40.8%	38.2%	3.84	0.176
2	504	211	41.8%	38.2%	3.84	0.339
3	381	132	34.6%	38.2%	3.84	0.339
4	98	28	28.5%	38.2%	3.84	2.72

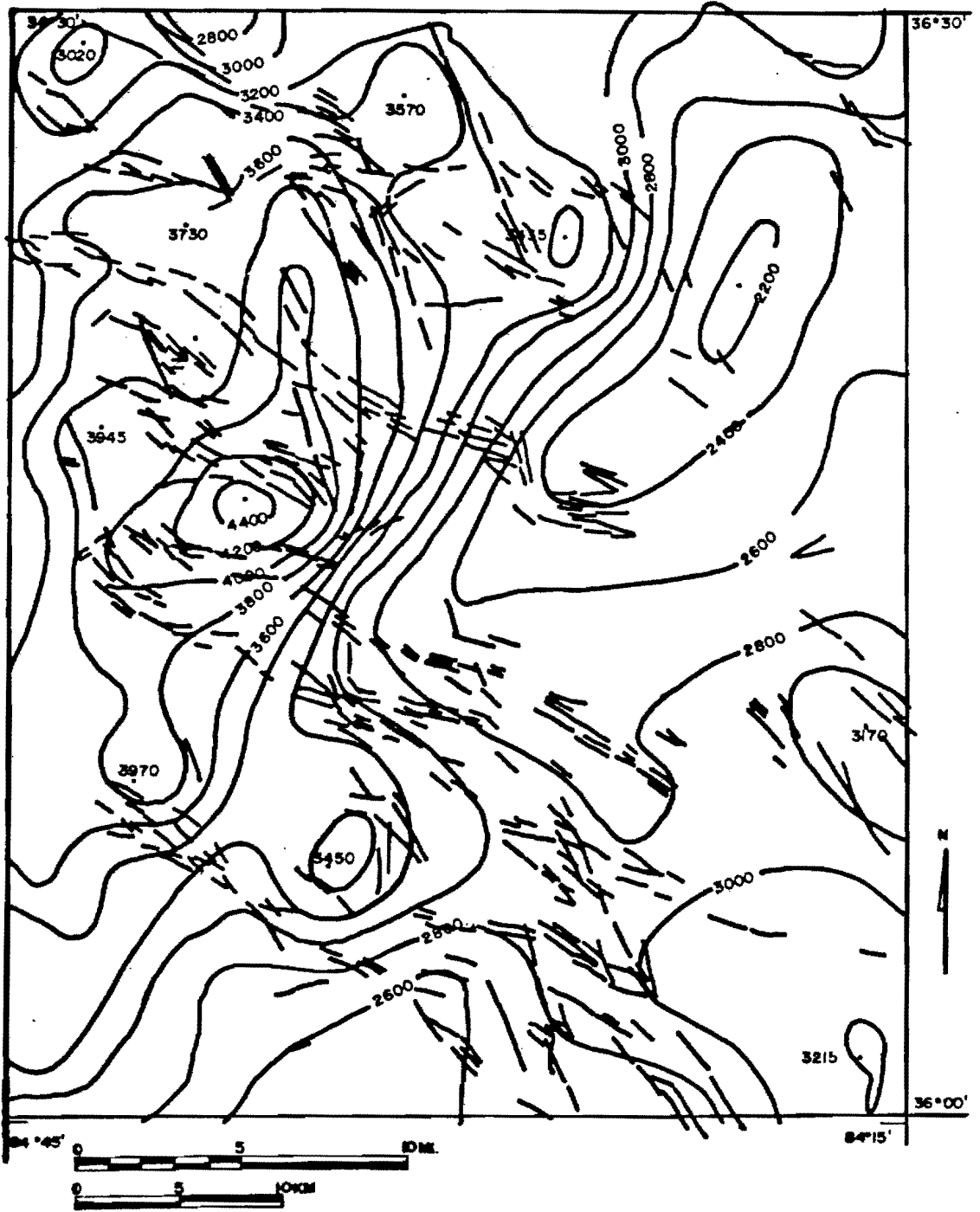


Figure 29. Lineaments aligned with aeromagnetic contours.

## CHAPTER VI

### HYDROCARBONS AND LINEAMENTS

#### INTRODUCTION

In the Powell Valley Anticline and the Pine Mountain Thrust Sheet, which are adjacent to the Wartburg Basin, production from gas wells is substantially greater where wells coincide closely with the intersection of lineaments (Miller, 1975, Miller et al., 1954 and Harris, 1976). Three phases of analysis were established to compare Seasat lineaments to oil and gas production and subsurface fracturing in wells.

#### I. PHASE 1: GENERAL ANALYSIS OF PRODUCTION IN 594 WELLS

A general study area was chosen in which 594 wells were analyzed (Figure 30). The wells were broken into two categories: 1) wells within 500 feet (152m) of a lineament, and 2) wells over 500 feet from a lineament. The wells were placed into four groups: a) gas producing wells, b) oil producing wells, c) combined gas and oil producing wells, and d) dry wells. Statistical analysis of the two categories is based on the following data (Table 12):

N: Number of wells per category

n: Number of wells per group

$n/N(100)$ : Percentage of wells per group

$n/N(100)_{exp}$ : Expected percentage of wells per group

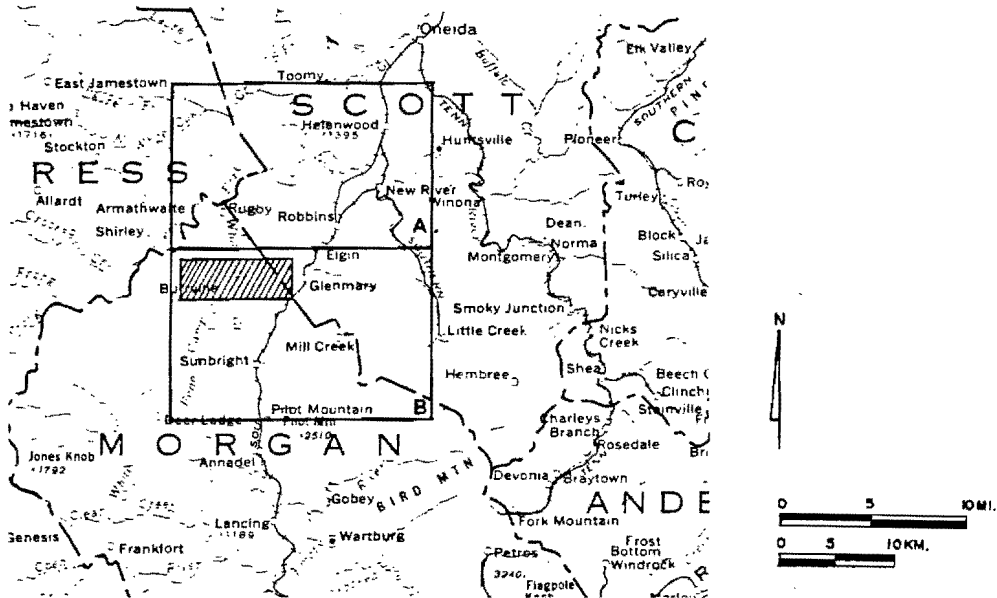


Figure 30. Study area for Phase 1 (Blocks A and B).

cv: Critical value (Chi square test)

cv-cal: Calculated critical value

Null hypothesis: The observed percentage of wells per group in each category equals the expected percentage of wells per group in each category.

Results: The null hypothesis was not rejected in any group by either category.

Conclusion: In this phase of analysis, the proximity of wells to lineaments does not indicate increased oil and gas production.

TABLE 12: Comparison of Wells Over 500 ft. from a Lineament to Wells Within 500 ft. of a Lineament

Categories and Well Groups	N Number of Wells per Category	n Number of Wells per Group	n/N(100) Percentage of Wells per Group	n/N(100)exp Expected Percentage of Wells per Group	cv critical value	cv-cal calculated critical value
Wells over 500 ft. from Lineaments						
Gas	372	98	26.3%	25%	3.84	0.067
Oil	372	110	29.5%	31.4%	3.84	0.114
Gas and Oil	372	83	22.3%	22.7%	3.84	0.007
Dry	372	81	21.7%	20.9%	3.84	0.030
Wells within 500 ft. of Lineaments						
Gas	222	50	22.5%	25%	3.84	0.250
Oil	222	77	34.6%	31.4%	3.84	0.326
Gas and Oil	222	52	23.4%	22.7%	3.84	0.021
Dry	222	43	19.5%	20.9%	3.84	0.666

## II. PHASE 2: ANALYSIS OF GAS AND OIL PRODUCTION IN 308 WELLS

In a more detailed analysis, initial hydrocarbon production of 308 wells in the general study area was analyzed. Information on these wells included the initial daily production, the date and length of the production test, and wellhead pressure at the end of the test (Tennessee Division of Geology, 1982). Wells were analyzed up to 1500 feet (457.5m) from lineaments and were placed into 4 categories: 1) average oil production with respect to distance from a lineament, 2) average gas production with respect to distance from a lineament, 3) average wellhead pressure for oil wells with respect to distance from a lineament, 4) average wellhead pressure for gas

wells with respect to distance from a lineament. A t-test (Morisawa, 1976) using a 0.05 level of significance (Guilford, 1956) was used to analyze each category.

Category 1: Initial oil production with respect to distance from a lineament

The statistical analysis was based on the following data (Table 13):

N: Number of wells per 100 ft. (30.4m) interval

X: Average well production per interval

Sum X: Total production per interval

SD: Standard Deviation

t-crit: Critical t value

t-cal: Calculated t value

Null hypothesis: There is no significant difference between production of oil wells within 100 feet (30.4m) of a lineament compared to wells over 100 feet from a lineament.

Results: The null hypothesis was rejected by three 100 ft. intervals: 100' to 200', 300' to 400', and 1300' to 1400'. The calculated t values for these three intervals slightly exceeds the t critical value. There is no significant increase in production for these three intervals.

Conclusions: When production averages for Category 1 are plotted (Figure 31) a very slight increase in oil production is indicated for wells more distant from a lineament although this increase is not backed up statistically.

TABLE 13: Comparison of Oil Production in Wells with Respect to Distance from Lineaments\*

Well Distance from Lineament	N Number of Wells	X Average Production per Well	Sum X Total Production	SD Standard Deviation	t-crit t value critical	t-cal t value calculated
0-100 ft.	19	104.1	1978	95.301		
100-200 ft.	10	35.6	356	39.608	2.052	2.099
200-300 ft.	11	128.4	1412	193.395	2.048	0.444
300-400 ft.	8	10.9	87	7.959	2.060	2.659
400-500 ft.	15	64.9	974	69.436	2.037	1.297
500-600 ft.	8	46.25	370	51.055	2.060	1.560
600-700 ft.	6	132.41	794.5	205.869	2.069	0.433
700-800 ft.	10	90.8	908	92.336	2.052	0.348
800-900 ft.	10	162.45	1624.5	216.028	2.052	0.970
900-1000 ft.	2	127	254	89.000	2.093	0.309
1000-1100 ft.	10	65.8	658	101.790	2.052	0.969
1100-1200 ft.	8	41.25	330	56.173	2.060	1.676
1200-1300 ft.	10	51.0	510	46.630	2.052	1.602
1300-1400 ft.	4	256.25	1025	183.145	2.080	2.288
1400-1500 ft.	5	44.8	224	36.972	2.074	1.306

\*Production is measured in Barrels of Oil Produced Daily (BOPD)

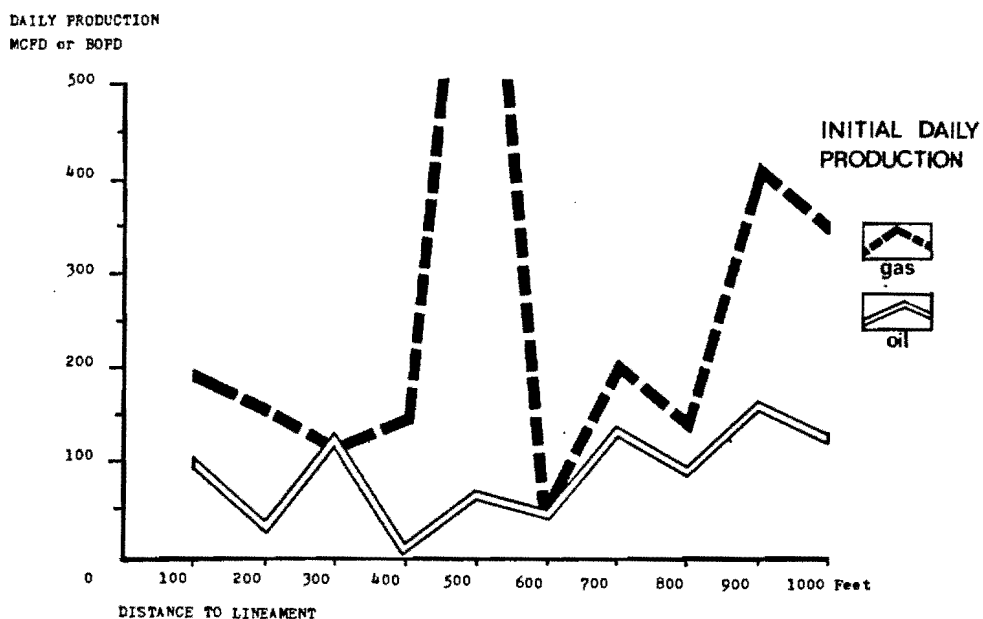


Figure 31. Initial oil and gas well production averages.



Category 2: Initial gas production with respect to distance from a lineament

A total of 120 gas wells were measured within 1500 feet (457.5m) of mapped lineament traces. Statistical analysis of production in these wells is based on the following data (Table 14):

N: Number of wells

X: Average production per well per interval

Sum X: Total production per interval

SD: Standard Deviation

t-crit: Critical t value

t-cal: Calculated t value

Null hypothesis: There is no significant difference between production of gas wells within 100 feet (30.4m) of a lineament compared to wells over 100 feet from a lineament.

Results: The null hypothesis is not rejected in any 100 ft. interval.

Conclusions: Statistically no significant increase in gas production occurs for wells closer to lineaments. When average well production per interval (X) is plotted, there is a slight trend towards increased production for wells farther from lineaments (Figure 31).

Category 3: Initial wellhead pressure for oil wells with respect to distance from a lineament

Data was available on initial wellhead pressure for 70 oil wells located within 1500 feet (457.5m) of mapped

TABLE 14: Comparison of Gas Production in Wells with Respect to Distance from Lineaments\*

Well Distance From Lineament	N Number of Wells	X Average Production per Well	Sum X Total Production	SD Standard Deviation	t-crit t value critical	t-cal t value calculated
0-100 ft.	20	198	3960	233.682		
100-200 ft.	8	159.4	1275	120.323	2.056	0.428
200-300 ft.	11	119	1309.5	81.293	2.045	1.050
300-400 ft.	10	146	1461	148.219	2.048	0.621
400-500 ft.	7	946	6625	1911.740	2.060	1.650
500-600 ft.	4	55	220	35.791	2.074	1.170
600-700 ft.	6	203	1219	197.019	2.064	0.52
700-800 ft.	8	146.5	1172	94.215	2.056	0.58
800-900 ft.	10	414	4141	592.716	2.048	1.38
900-1000 ft.	9	351.8	3167	299.728	2.052	1.44
1000-1100 ft.	9	450	4052	638.503	2.052	1.49
1100-1200 ft.	6	36	217	20.301	2.064	1.63
1200-1300 ft.	7	191.5	1340.25	340.878	2.060	0.12
1300-1400 ft.	2	174.5	349	49.5	2.086	0.14
1400-1500 ft.	3	29	87	17.720	2.080	1.19

\*Production is measured in Thousands of Cubic Feet of Gas Produced Daily (MCFD)

lineaments. The following statistical data were used (Table 15):

N: Number of wells per 100 ft. (30.4m) interval

X: Average wellhead pressure per interval

Sum X: Total production per interval

SD: Standard Deviation

t-crit: Critical t value

t-cal: Calculated t value

Null hypothesis: There is no significant difference between wellhead pressure of oil wells within 100 feet (30.4m) of a lineament compared to wellhead pressure of oil wells over 100 feet from lineaments.

Results: The null hypothesis was not rejected in any 100 ft. interval.

Conclusions: When average wellhead pressures are graphed (Figure 32), a very slight increase in wellhead pressure is indicated for wells farther from lineaments.

TABLE 15: Comparison of Oil Wellhead Pressure with Respect to Well Distance From a Lineament\*

Well Distance From Lineament	N Number of Wells	X Average Pressure per Well	SD Standard Deviation	t-crit t value critical	t-cal t value calculated
0-100 ft.	14	235.35	151.710		
100-200 ft.	3	98.33	51.045	2.131	1.452
200-300 ft.	10	200.8	223.064	2.074	0.432
300-400 ft.	2	142.5	32.5	2.145	0.807
400-500 ft.	7	239.28	160.143	2.093	0.054
500-600 ft.	4	151	63.585	2.120	1.023
600-700 ft.	3	180	42.426	2.131	0.588
700-800 ft.	6	195.83	163.106	2.101	0.495
800-900 ft.	2	300	120.00	2.145	0.540
900-1000 ft.	1	410	0.0	2.160	1.071
1000-1100 ft.	6	206.66	112.608	2.101	0.395
1100-1200 ft.	3	433.3	62.361	2.131	2.085
1200-1300 ft.	5	214.2	84.632	2.111	0.279
1300-1400 ft.	2	437.15	37.5	2.145	1.755
1400-1500 ft.	2	292.5	47.5	2.145	0.494

\*Pressure is measured in pounds per square inch (psi)

Category 4: Initial wellhead pressure for gas wells with respect to distance from a lineament

Initial wellhead pressure was available for 66 gas wells located within 1500 feet (457.5m) of lineaments. Statistical analysis was based on the following data (Table 16):

N: Number of wells per 100 ft. (30.4m) interval

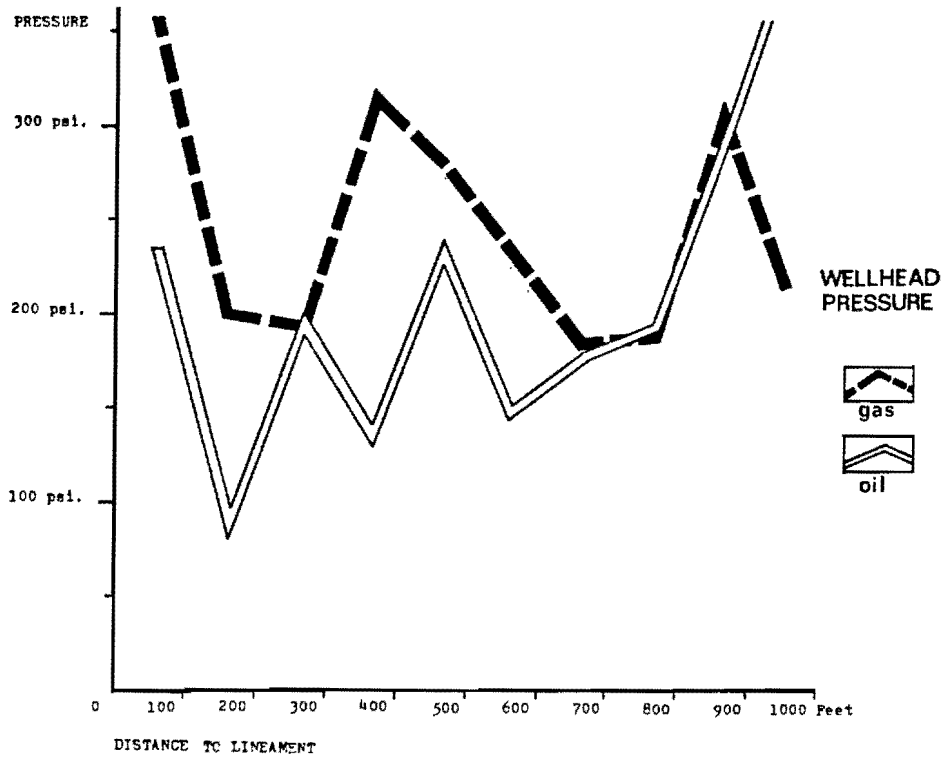


Figure 32. Initial wellhead pressure averages.

X: Average wellhead pressure per interval

SD: Standard Deviation

t-crit: Critical t value

t-cal: Calculated t value

Null hypothesis: There is no significant difference between wellhead pressure of gas wells within 100 feet (30.4m) of lineaments compared to wellhead pressure of gas wells over 100 feet from lineaments.

Results: The null hypothesis was rejected by the 1000' to 1100' interval. The other intervals do not reject the null hypothesis.

TABLE 16: Comparison of Gas Wellhead Pressure with Respect to Well Distance from a Lineament\*

Well Distance From Lineament	N Number Wells	X Average Pressure per Well	SD Standard Deviation	t-crit t value critical	t-cal t value calculated
0-100 ft.	12	357	220.416		
100-200 ft.	4	201.25	141.438	2.145	1.239
200-300 ft.	7	196.43	98.930	2.111	1.725
300-400 ft.	5	319	157.715	2.131	0.328
400-500 ft.	3	283.33	144.299	2.160	0.512
500-600 ft.	3	238.66	123.990	2.130	0.833
600-700 ft.	4	187.5	94.439	2.145	1.396
700-800 ft.	2	190	40.0	2.179	0.989
800-900 ft.	6	313.3	211.511	2.120	0.378
900-1000 ft.	6	216.66	73.270	2.120	1.427
1000-1100 ft.	5	121.2	63.022	2.131	2.209
1100-1200 ft.	2	180	0.0	2.179	1.051
1200-1300 ft.	4	290	100.062	2.145	0.550
1300-1400 ft.	2	212.5	27.5	2.179	0.857
1400-1500 ft.	1	185	0.0	2.201	0.689

\*Pressure is measured in pounds per square inch (psi)

Conclusions: The calculated t value exceeds the critical t value by a very small margin in the 1000' to 1100' interval. Statistically this does not indicate a significant trend towards increased wellhead pressure. When the pressure averages were graphed there is no clear indication of increased pressure in wells farther from lineaments.

### III. PHASE 3: SUBSURFACE FRACTURING IN RELATION TO LINEAMENTS

Although lineaments were observed as topographic features in this study, an analysis of fracturing at depth using information provided from well logs could give an indication of the subsurface expression of lineaments. Well logs from

25 wells in the Union Hill Field area, north of Sunbright, Tennessee were examined for fractures, porosity zones, and related oil and gas pays. These were then related to lineaments mapped from Seasat imagery of the area (Figure 33). Using the compensation log portion of the well log, fracture density was analyzed in two of the main oil and gas producing formations in the area, the Hartselle Formation and the Monteagle Limestone (Burwell et al, 1967)

The Hartselle Formation, which occurs at depths from 1050 to 1290 feet (320m to 393m) depending on elevation, is composed of a fine to medium grain, quartzitic sandstone that is often clear and subrounded. Average thicknesses in the area range from 10 to 25 feet (3.04m to 7.62m). This formation usually contains at least one major fracture and has a density porosity ranging from 5% to 40%.

The main oil and gas producing formation, occurring just below the Hartselle Formation, is the Monteagle Limestone. This limestone, which averages 200 to 220 feet thick (60.9m to 67m), is fine to medium grained, contains fossil fragments, and has oolitic zones up to 30 feet (9.1m) thick. The oolitic zones, which are often fractured, have up to 25% porosity. Wells drilled in the Union Hill area average 1300 feet to 1500 feet (396m to 457m) in depth with a few wells being drilled to 1800 feet (548.6m) into the Fort Payne Formation.

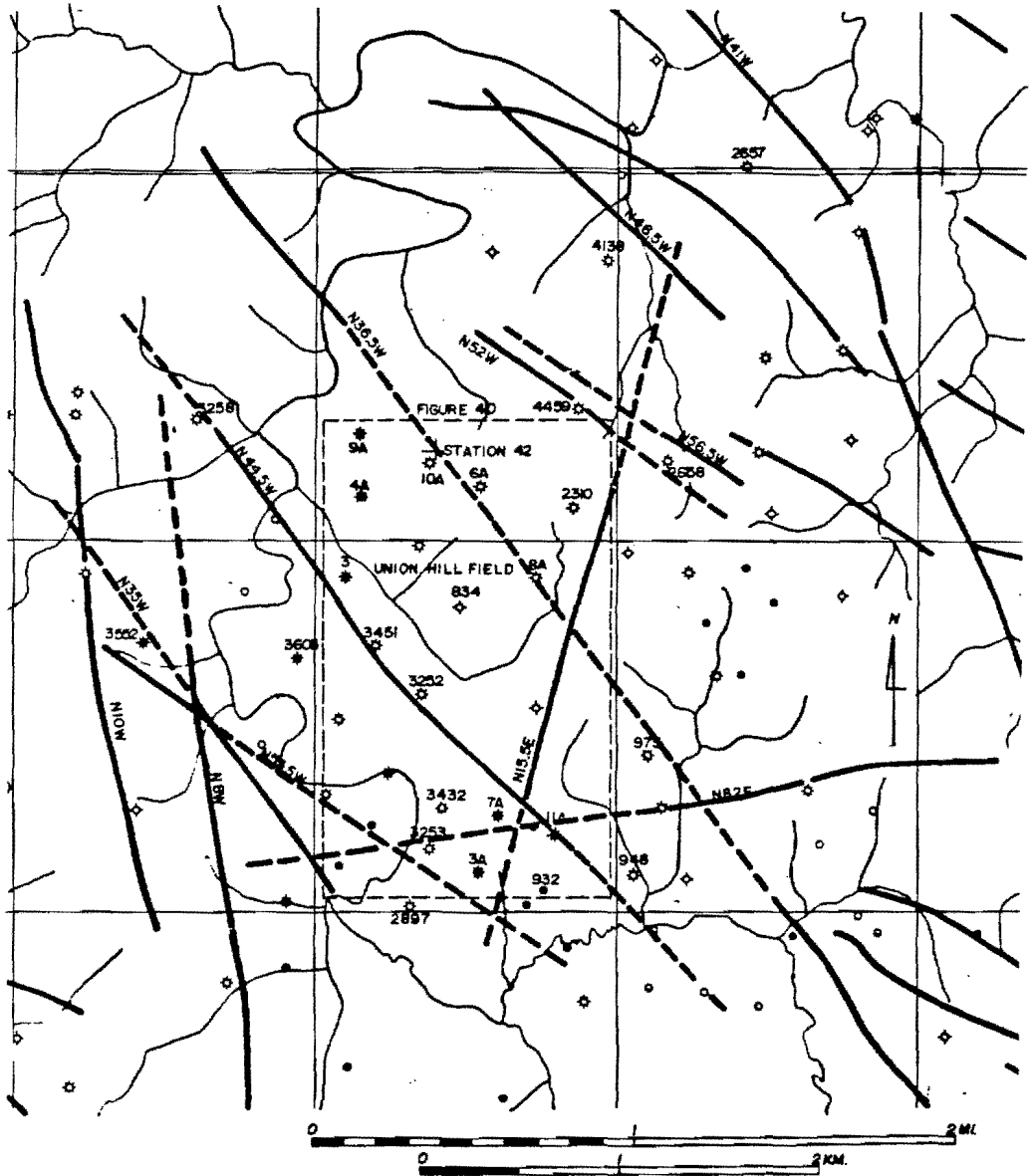


Figure 33. Map showing the locations of 25 wells analyzed for fracturing at depth. Lineament locations and orientations are indicated. Dashed lines indicate probable lineament traces.

The 25 wells were statistically analyzed in three categories: 1) average number of fractures per well in relation to distance from a lineament, 2) average number of hydrocarbon bearing fractures per well in relation to distance from a lineament, 3) average number of fractures and pay fractures per well in relation to lineament orientation.

Category 1: Average number of fractures per well in relation to distance from a lineament

Using the compensation logs, 133 fractures were observed in the Hartselle Formation and the Monteagle Limestone. Ten different lineaments were considered in relation to the well fractures. Each well was correlated to the closest lineament. The t-test (Morisawa, 1976) using a 0.05 level of significance (Guilford, 1956) was used for Categories 1 and 2. Statistical analysis for this category is based on the following data (Table 17):

N: Number of wells per 100 ft. (30.4m) interval

X: Average fractures per well per interval

Sum X: Total fractures per interval

SD: Standard Deviation

t-crit: Critical t value

t-cal: Calculated t value

Null hypothesis: There is no significant difference between the average number of fractures in wells within 100 feet of lineaments compared to wells over 100 feet from lineaments.



Results: The null hypothesis was rejected by the 100' to 200', the 600' to 700', the 900' to 1000', and the Over 1000' intervals. The calculated t values were significantly higher than the critical t values for all these intervals except the 600' to 700' interval.

Conclusions: Wells have a significantly greater amount of subsurface fracturing with increasing distance from lineaments. When the average fractures per well per interval were graphed, a significant trend towards increased fracturing in wells farther from lineaments is also indicated (Figure 34).

Category 2: Average number of hydrocarbon bearing fractures per well in relation to distance from a lineament

Of the total 133 fractures in 25 wells, 59 fractures (44.3%) had some indication of a gas or oil emission on the well logs. Statistical analysis in this category is based on the following data (Table 18):

N: Number of wells per 100 ft. (30.4m) interval

X: Average number of pay fractures per well per interval

Sum X: Total number of pay fractures per interval

SD: Standard Deviation

t-crit: Critical t value

t-cal: Calculated t value

Null hypothesis: There is no significant difference in the

TABLE 17: Comparison of Well Fractures with Respect to Distances from Lineaments

Well Distance From Lineament	N Number of Wells	X Average Fractures per Well	Sum X Total Fractures	SD Standard Deviation	t-crit t value critical	t-cal t value calculated
0-100 ft.	5	5	25	2.756		
100-200 ft.	5	8.8	44	0.979	1.901	8.154
200-300 ft.	2	7.5	15	2.500	2.001	0.841
300-400 ft.	2	8.5	17	3.500	2.042	0.315
400-500 ft.	2	8.5	17	0.500	2.041	0.0
500-600 ft.	2	7.5	15	4.500	2.042	0.880
600-700 ft.	1	10	10	0.0	2.069	2.175
700-800 ft.	0	-	-	-	-	-
800-900 ft.	1	6	6	0.0	0.0	0.0
900-1000 ft.	2	10.5	21	1.500	2.060	7.075
Over 1000 ft.	2	11.0	22	1.000	2.020	4.065

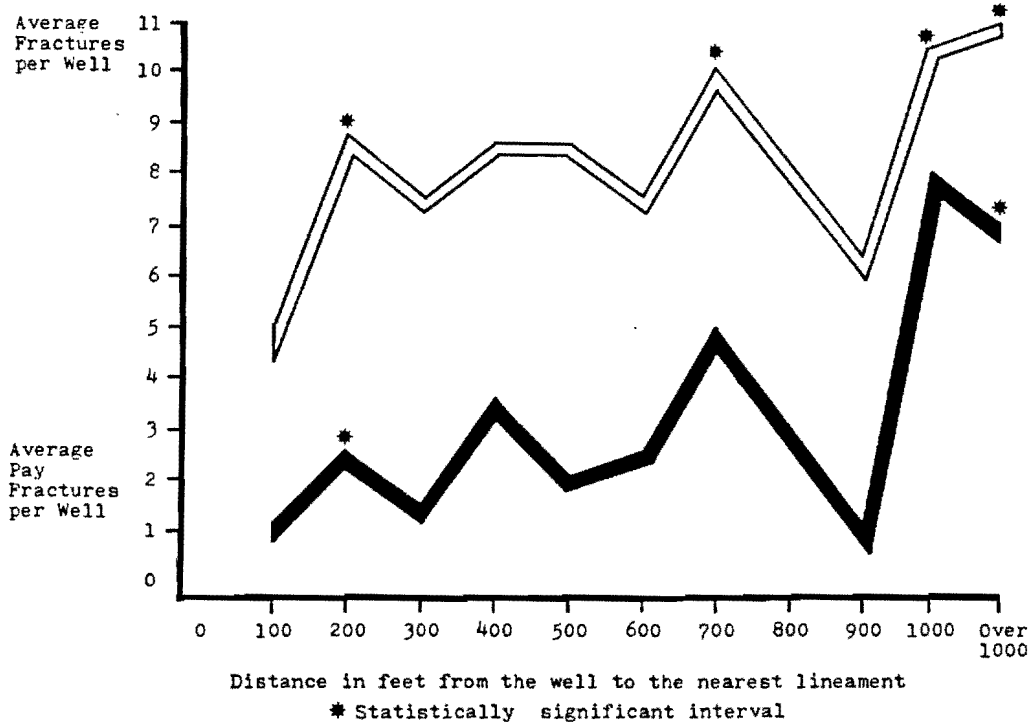


Figure 34. Average fractures and pay fractures per well in relation to distance from a lineament.

average number of oil and gas producing fractures in wells within 100 feet of lineaments compared to the average number of oil and gas producing fractures in wells over 100 feet from lineaments.

Results: The null hypothesis was rejected by two intervals, the 100' to 200' and the Over 1000' interval.

Conclusions: A slight statistical trend indicates that wells have more pay fractures farther from lineaments. When the average number of pay fractures per well were graphed (Figure 34), there is also an indication towards more pay fractures with increasing distance from lineaments.

TABLE 18: Comparison of Well Fractures Containing Oil and Gas with Respect to Distances from Lineaments

Well Distance From Lineament	N Number of Wells	X		SD Standard Deviation	t-crit t value critical	t-cal t value calculated
		Average Pay Fractures per Well	Sum S Total Pay Fractures			
0-100 ft.	5	1.2	6	0.748		
100-200 ft.	5	2.6	13	1.356	2.110	2.243
200-300 ft.	2	1.5	3	0.500	2.145	1.295
300-400 ft.	2	3.5	7	1.500	2.306	1.982
400-500 ft.	2	2	4	0.0	2.262	1.134
500-600 ft.	2	2.5	5	2.500	2.365	0.236
600-700 ft.	1	5	5	0.0	2.306	2.000
700-800 ft.	0	-	-	-	-	-
800-900 ft.	1	1	1	0.0	0.0	0.0
900-1000 ft.	2	4	8	0.0	3.182	0.0
Over 1000 ft.	2	3.5	7	0.500	2.160	2.645

Category 3: Average number of fractures and pay fractures per well with respect to lineament orientation

The 25 wells were also examined to determine if a greater number of fractures and pay fractures were associated with a particular lineament orientation. Statistical analysis was made using the Chi square test (Ambrose et al., 1977) with a 0.05 level of significance (Steel et al., 1960). The following data were used (Tables 19 and 20):

N: Number of wells per orientation

F: Number of fractures or pay fractures per well per orientation

F/N: Average number of fractures or pay fractures per well per orientation

F/N exp: Expected average number of fractures or pay fractures per well per orientation

cv: Critical value

cv-cal: Calculated critical value

Null hypothesis: The observed number of fractures or pay fractures per well per orientation equals the expected number of fractures or pay fractures per well per orientation.

Results: The null hypothesis was not rejected in any lineament orientation either in the fractures group or the pay fractures group.

Conclusions: No significant relationship exists between lineament orientations and fracturing or pay fracturing.

TABLE 19: Comparison of Well Fractures with Lineament Orientations

Lineament Orientation	N Number of Wells per Orientation	F Number of Fractures per Well	F/N Average Fractures per Well	F/N exp Expected Average Fractures per Well	cv critical value	cv-cal calculated critical value
N56.5 <sup>o</sup> W	1	5	5	7.72	16.9	0.958
N55.5 <sup>o</sup> W	1	10	10	7.72	16.9	0.673
N52 <sup>o</sup> W	1	5	5	7.72	16.9	0.958
N46.5 <sup>o</sup> W	1	3	3	7.72	16.9	2.885
N44.5 <sup>o</sup> W	8	63	7.87	7.72	16.9	0.002
N41 <sup>o</sup> W	1	9	9	7.72	16.9	0.212
N36.5 <sup>o</sup> W	5	39	7.8	7.72	16.9	0.046
N35 <sup>o</sup> W	1	8	8	7.72	16.9	0.010
N15.5 <sup>o</sup> E	1	8	8	7.72	16.9	0.010
N82 <sup>o</sup> E	2	20	10	7.72	16.9	0.673

TABLE 20: Comparison of Well Fractures Containing Oil and Gas with Lineament Orientations

Lineament Orientation	N Number of Wells per Orientation	F Number of Pay Fractures per Orientation	F/N Average Pay Fractures per Well per Orientation	F/N exp Expected Average	cv critical value	cv-cal calculated critical value
N56.5 <sup>o</sup> W	1	1	1	2.36	16.9	0.783
N55.5 <sup>o</sup> W	1	5	5	2.36	16.9	2.953
N52 <sup>o</sup> W	1	2	2	2.36	16.9	0.54
N46.5 <sup>o</sup> W	1	0	0	2.36	16.9	2.36
N44.5 <sup>o</sup> W	8	19	2.375	2.36	16.9	0.00
N41 <sup>o</sup> W	1	4	4	2.36	16.9	1.13
N36.5 <sup>o</sup> W	5	9	1.8	2.36	16.9	0.132
N35 <sup>o</sup> W	1	3	3	2.36	16.9	0.173
N15.5 <sup>o</sup> E	1	2	2	2.36	16.9	0.054
N82 <sup>o</sup> E	2	7	3.5	2.36	16.9	0.550

## CHAPTER VII

### CONCLUSIONS

Lineaments from Seasat imagery were located in the field with a high degree of accuracy. 70% of all imagery lineaments that were investigated were located. 10% of these proved to be man-made linear features such as power line right-of-ways and roads. Lineaments in bedrock exposures were usually within 50 feet (15.2m) of where they appeared on the imagery. The presence of moisture in the lineament zone was found to increase the probability that a lineament would appear on the imagery. Missing segments of lineaments often coincided with recently cultivated areas.

Although only 2% of the lineaments from aerial photographic imagery matched with lineaments from Seasat imagery, portions of lineaments that were missing on one type of imagery were often filled in by lineaments from the other type of imagery. Probable lineament lengths were also extended in this manner. One out of every six lineaments that stop on one type of imagery were found to be terminated by a crosscutting lineament from the other type of imagery. Statistical analysis proved that Seasat lineaments are longer than aerial photographic lineaments. This could indicate that Seasat detects portions of lineaments that are not visible on aerial photographic imagery.

Seasat imagery combined with Landsat imagery has recently become commercially available (Aero Service, 1982). Hopefully this type of imagery will give an insight into lineament trends.

1186 lineaments in the study area were divided into 4 systems based on orientation. The difference between System 1 and the other three systems is statistically significant in three out of six categories used in this analysis. System 1 lineaments are longer than Systems 2, 3, and 4. They show a closer relationship to major drainage in the area, and they are involved in more crosscutting lineament terminations than Systems 2 and 3. System 1 lineaments may represent a macro lineament system which extends completely thru the Wartburg Basin. A macro lineament system with the same characteristics has been found in northern Alabama (Drahovzal, 1975).

Statistically, no evidence proves that wells closer to lineaments had a higher initial hydrocarbon production or wellhead pressure. When production averages in relation to well distance from a lineament are graphed, a slight trend occurs towards increased production for wells located far from lineaments. Statistical evidence indicates a slight trend towards increased fracturing in wells farther from lineaments. This evidence is also confirmed by graphs showing average well fractures with respect to distance from a lineament.

Imagery from a more refined synthetic aperture radar system on the second Space Shuttle mission (1981) will soon be publicly available. This imagery will be "tuned" to give the highest resolution with the least possible distortion. In the future, Seasat-type imagery combined with other types of imagery from Landsat IV and the Space Shuttle will give a more accurate insight into lineament trends and their relationship to the topography.



LIST OF REFERENCES

## LIST OF REFERENCES

- Aero Service, 1982, Sarsat imagery: Photogrammetric Engineering and Remote Sensing, vol. 48, no. 9, p.1403
- Ambrose, H.W. III, and Ambrose, K.P., 1977, A handbook of biological investigation: Hunter Publishing Co., Winston-Salem, N.C.
- Barlow, J. A., 1969, Stratigraphy and paleobotany of the youngest Pennsylvania strata in the Caryville, Tennessee area: Unpublished doctoral dissertation, The University of Tennessee, Knoxville.
- Blanchet, P.D., 1957, Development of fracture analysis as exploration method: Bulletin of American Association of Petroleum Geologists, v. 41, no. 8, pp. 1748-1759.
- Burwell, H.B., and Milhous, H.C., 1967, Oil and gas map, Morgan County, Tennessee: State of Tennessee Dept. of Conservation, Division of Geology.
- Daily, M.I., Farr, T., and Elachi, C., 1979, Geologic interpretation from composited radar and Landsat imagery: Photogrammetric Engineering and Remote Sensing, vol. 45, no. 8, pp. 1109-1116.
- Drahovzal, J.A., Neathery, T.L., and Wielchowsky, C.C., 1975, Significance of selected lineaments in Alabama: Third Earth Resources Technology Satellite-1 Symposium, Vol. I: Technical Presentations, Sec. A., Paper G-24, SP-351, pp. 987-918.
- Elachi, C., 1980, Space borne imaging radar: geologic and oceanographic applications: Science, vol. 209, no. 4461, pp. 1073-1082.
- Ford, J.P., Blom, R.G., Bryan, M.L., Daily, M.I., Dixon, T.H., Elachi, C., Xenos, E.C., 1980, Seasat views North America, the Caribbean, and Western Europe with imaging radar: NASA, Jet Propulsion Laboratory, Pub 80-67, 141 p.
- Ford, J.P., 1980, Seasat orbital radar imagery for geologic mapping: Tennessee-Kentucky-Virginia: AAPG Bull., vol. 64, no. 12., pp. 2064-2094.
- Foster, J.L., and Hall, D.K., 1981, Multisensor analysis of hydrologic features with emphasis on the Seasat SAR: Photogrammetric Engineering and Remote Sensing, vol, 47, no. 5, pp. 655-664.

- Guilford, J.P., 1956, Fundamental statistics in psychology and education: McGraw-Hill Book Company, New York.
- Halbouty, M.T., 1976, Application of Landsat imagery to petroleum and mineral exploration: Bulletin of the American Association of Petroleum Geologists, v. 60, no. 5, pp. 745-793.
- Hardeman, W.D., 1966, Geologic map of Tennessee, East Central Sheet, G.A. Swingle, R.A. Miller, E.T. Luther, D.S. Fullerton, C.R. Sykes, R.K. Garman (compilers and editors): Tennessee Department of Conservation, Division of Geology.
- Harris, L.D., 1976, Thin-skinned tectonics and potential hydrocarbon traps illustrated by a seismic profile in the Valley and Ridge Province of Tennessee: U.S. Geological Survey Journal of Research, vol. 4, pp. 379-386.
- Hobbs, W.H., 1911, Repeating patterns in the structure of the land: Geological Society of America Bulletin, v. 22, pp. 123-176.
- Kaiser, E.P., 1950, Structural significance of lineaments: (abs.) Geological Society of America Bulletin, v. 61, no. 12, pp. 1475-1476.
- Lattman, L.H., 1958, Technique of mapping geologic fracture traces and lineaments on aerial photography: Photogrammetric Engineering, vol. 24, no. 4, pp. 568-576.
- Lattman, L.H. and Nickelson, R.P., 1958, Photogeologic fracture trace mapping in the Appalachian Plateau: Bulletin of the American Association of Petroleum Geologists, v. 42, no. 9, pp. 2238-2245.
- Luther, E.T., 1959, The coal reserves of Tennessee: Tennessee Division of Geology Bulletin no. 63., 294 p.
- Masuoka, P.L., 1981, Analysis of photogeologic fracture traces and lineaments in the northern portion of the Wartburg Basin, Tennessee: Unpublished Master's thesis, The University of Tennessee, Knoxville.
- Miller, R.L., 1975, Oil and gas from the Upper and Middle Ordovician rocks in the Appalachian Basin: U.S. Geological Survey Misc. Inv. Map I-917-C.

- Miller, R.L., and Fuller, J.O., 1954, Geology and oil resources of the Rose Hill District- the fenster area of the Cumberland Overthrust Block: Lee County, Virginia: Virginia Geological Survey Bulletin 71, 374 p.
- Morisawa, M., 1976, Geomorphology laboratory manual: John Wiley and Sons, Inc., New York, 253 p.
- NASA, 1980, Resolution and Coverage: Keys to Planetary Studies: Jet Propulsion Laboratory Publication, 630-10, 44 p.
- Nickelson, R.P. and Hough, V.D., 1967, Jointing in the Appalachian Plateau of Pennsylvania: Geological Society of America Bulletin, v. 78, pt. 1, pp. 609-629.
- NOAA, 1980, Seasat SAR optical and digital data: U.S. Department of Commerce, Environmental Data and Information Service, National Climatic Center., Satellite Services Division., Washington, D.C., 20 p.
- Schmugge, T.J., 1980, Microwave approaches in hydrology: Photogrammetric Engineering and Remote Sensing, vol. 46, no. 4, pp. 495-507.
- Secor, D.T., Jr., 1965, Role of fluid pressure in jointing: American Journal of Science, v. 263, p. 633-646.
- Slusarski, M.L., 1979, Photogeologic fracture traces and lineaments in the Wartburg Basin section of the Cumberland Plateau Physiographic Subprovince, Tennessee: Unpublished Master's thesis, The University of Tennessee, Knoxville.
- Smith, W.W., and Drahovzal, J.A., 1972, Possible geo-fracture control of ore deposition in Alabama: Society of Mining Engineers of AIME, Preprint No. 72-H-316, 8 p.
- Steel, R.G.D., and Torrie, J.H., 1960, Principles and procedures of statistics: McGraw-Hill Book Co., New York.
- Tennessee Department of Conservation, 1981, Well location index map, Scott and Morgan Counties, Division of Geology.
- \_\_\_\_\_, 1982, Completions, well production report, computer listing, Scott and Morgan Counties, Division of Geology.

- Watkins, J.S., 1964, Regional geologic implications of the gravity and magnetic fields of a part of Eastern Tennessee and Southern Kentucky: Geological Survey Professional Paper 516-A, 17 p.
- Wilson, C.W., 1949, Pre-Chattanooga stratigraphy in Central Tennessee: Tennessee Department of Conservation, Division of Geology Bulletin 56, 407 p.
- Wilson, J.T., 1965, A new class of faults and bearing on continental drift: Nature, vol. 207, pp. 343-347.

## APPENDIX

## GLOSSARY

Terms which are commonly employed in remote sensing and relate to Seasat (after Ford, 1980):

active sensor-Any remote sensing system that provides its own source of energy to illuminate a scene or target and measures the reflectance of that energy.

azimuth-Bearing of a line measured clockwise from geographic north; for example,  $150^{\circ}$ , to denote the direction of sun illumination.

azimuth (radar imaging)-Along-track direction of image acquisition.

backscatter (radar)-Portion of transmitted microwave energy that is reflected to the radar antenna to create a radar image.

backslope-Slope that is inclined away from an incident radar beam.

band-An interval in the electromagnetic spectrum whose boundaries are marked by a lower and an upper limiting wavelength or frequency.

correlation (radar)-Processes by which the Doppler phase histories recorded on tape or radar signal film are converted into radar images, using optical or digital techniques.

foreslope-Slope that is inclined toward an incident radar beam.

ground resolution-The minimum distance between two adjacent features on the ground, or the minimum size of a feature on the ground, which can be detected by an imaging system.

incidence angle (radar)-Angle between the incident radar beam on the ground and the normal to the ground surface at a point of incidence.

Landsat-Any of a series of orbital imaging satellites that measure and record reflectance from the earth's surface at visible and infrared wavelengths.

layover (radar)-Geometric displacement of the top of a feature toward the near range on radar imagery.

look angle (radar)-Angle between the vertical plane and the line that links an imaging-radar antenna to a feature on the ground. Preferred measurement for spaceborne imaging radars.

look direction (radar)-Direction in which pulses of microwave energy are transmitted from an imaging-radar antenna; normally at right angles to the line of flight of the imaging platform.

microwave-Any electromagnetic wave having a wavelength in the interval between 1mm and 1m.

MSS-Multispectral scanner

multispectral scanner-An airborne or spaceborne imaging system that acquires images by scanning a scene in several wavelengths simultaneously.

radar-Radio detection and ranging. Radar is used in remote sensing for measuring and mapping earth and planetary surfaces

RBV-Return-beam vidicon.

real-aperture radar-A side-looking airborne imaging system in which for any given wavelength the resolution in the azimuth direction is determined by the physical length of the antenna, and the resolution in the range direction decreases progressively downward. The radar backscatter is recorded directly to form images.

SAR-Synthetic-aperture radar.

Seasat-An earth-orbiting satellite equipped with five instruments for studying ocean dynamics, including a side-looking synthetic-aperture imaging radar system. The satellite was launched in June 1978. All remote sensing capabilities failed on board in October 1978.

shadow (radar)-Area of no radar backscatter on an image. Caused by a ground feature which obstructs the radar beam and prevents illumination of the area behind it.

synthetic aperture radar-A side-looking airborne or spaceborne imaging system which uses the Doppler principle to sharpen the effective beamwidth of the antenna. The result is improved resolution in the azimuth



direction and constant resolution in the range direction. The radar backscatter is recorded on tape or on film and must be digitally or optically processed to form radar images.

## VITA

S.E.A. Brite was born in Memphis, Tennessee on July 25, 1949. He attended Catholic High School, graduating in 1967.

He enlisted in the U.S. Navy in 1967 and worked as a Spanish linguist for the Naval Security Group Activity until 1971. In the fall of 1973, Mr. Brite entered the University of Tennessee School of Architecture, obtaining a Bachelor of Architecture Professional Degree in 1977. In 1978, Mr. Brite entered the University of Tennessee School of Geology for graduate work. He is a member of the American Society of Photogrammetry, the American Association of Petroleum Geologists, the Geological Society of America, and the Tennessee Oil and Gas Association.

Since 1981, Mr. Brite has been self-employed as a consultant geologist specializing in oil and gas exploration. His work is centered in the Southeast. Portions of this thesis were presented at the annual meeting of the Tennessee Oil and Gas Association in May, 1982. A paper prepared from this talk will be published by the Tennessee Division of Geology in 1983.